• U C •

FCTUC FACULDADE DE CIÊNCIAS
E TECNOLOGIA
UNIVERSIDADE DE COIMBRA

Diogo da Encarnação Martins

A Circuit based on Communication Systems for Anesthesia Monitoring

Dissertação apresentada à Universidade de Coimbra para cumprimento dos requisitos necessários à obtenção do grau de Mestre em Engenharia Biomédica

Supervisors:
Professor Doctor César Alexandre Domingues Teixeira (CISUC,DEI)
Professor Doctor Alberto Jorge Lebre Cardoso (CISUC,DEI)

Coimbra, 2015

This work was developed in collaboration with

Center for Informatics and Systems (CISUC), Department of Informatics Engineering, University of Coimbra

Acknowledgments

First and foremost, I would like to thank my supervisor, Doctor César Teixeira, for all of the support, availability and motivation throughout the past year. His guidance and suggestions haven been constructive and contributed greatly to my research. I am also grateful to my co-supervisor, Doctor Alberto Cardoso, for the continued support and involvement in the development of my work. Their unlimited willingness to give their knowledge inspired me to pursue any possible solution to solve any step back and never give up in a face of a difficult challenge.

Moreover, I also thank Nuno Lopes and the Doctor Piedade Costa Gomes, from the Anesthesiology Unit of the Centro Hospitalar e Universitário de Coimbra, for the creation and provision of the EEG signals database.

I would like to thank my girlfriend, Filipa Figueiredo, for her smiles, caring and patience during hard times. Her love, kindness and encouragement that taught me to always look on the bright side.

I must highlight those who took part of my journey in Coimbra, for their friendship and truthful kindness. Carolina Silveira, Daniel Osório, Mariana Nogueira, Inês Barroso, Heloísa Sobral, Bruna Nogueira, Ricardo Simões, Luís Henriques, Ricardo Mendes and Pedro Duarte for showing me that dedication, humility, compassion and honesty are always rewarded. Also, for their expert ability to bring excitement, happiness and extreme weirdness to all of our friendly moments.

A special gratitude to my fellow choir singers from Orfeon Académico de Coimbra for making the past three years even more special and allowing me to experience unique opportunities.

A special thanks to Diogo Passadouro for his honesty, courage and persistence in believing in me, even when I wouldn't. Also, for his tireless friendship and confidence, and for always standing by my side when I needed.

But most of all I want to thank my family, specially my mother, for their unconditional support during my academic journey.

To these extraordinary people, for making and showing me who I am and encouraging be to be myself, I will be forever grateful.

"Perfection is achieved not when there is nothing more to add, but when there is nothing left to take away"

Antoine de Saint-Exupéry, *Le Petit Prince*

Abstract

In current surgical procedures, an incidence of approximately 0.2% of intraoperative awareness incidents, due to inadequate anesthesia, have been reported. A considerable amount of these reports result in psychiatric disorders. On the other hand, excessive anesthesia has been proven to increase postoperative recovery times and complications.

One of the main challenges that Medicine has faced is the correct monitoring of depth of anesthesia. Several monitoring methods have been presented through the years, the majority of them based on visual evaluations and lacking on objectivity.

More recently a more reliable set of monitors have been developed based on the recording of several biological signals. Since it has been shown that brain activity alters during general anesthesia, the most studied monitors are based on the monitoring of the brain's electrical activity through electroencephalogram (EEG).

In this thesis we developed from scratch a methodology that uses a usual telecommunications systems' technology to track frequency variations in EEG signals of patients under general anesthesia. The technology is based on a phase-locked loop (PLL) circuit incorporating a preprocessing subcircuit that helps remove interferences and prepares the EEG signal to comply with the requirements. This devices allows for a real-time estimation of frequency components, without requiring signal windowing. This has great advantages from a spectral analysis point-of-view since it minimizes the risk of frequency leakage.

It was found that the designed circuit, for single frequency signals, presented a hold range of $\pm 55Hz$ enough to cover the desired frequency range of an EEG and could track abrupt frequency variations of $\pm 20Hz$. However, it was also found, with the Simulink model, that for mixed signals (several frequency components) the circuit locks into different components depending on the VCO's initial frequency. The same conclusions could not be observed in analog implementation, due to lack of time. However, we believe that the results of the Simulink model would be reproduced by the implemented physical circuit.

Key words Phase-Locked Loops (PLL), Anesthesia monitoring, Depth of Anesthesia (DOA), Electroencephalogram (EEG), Frequency tracking, analog circuits.

Resumo

Atualmente, cerca de 0.2% das cirugias realizadas registam casos de pacientes com consicência intraoperativa devido a uma dosagem inadequada de anestesia. Grande parte destes casos resultam em transtornos psicológicos. Por outro lado, doses excessivas de anestesia resultam num aumento de tempo de recuperação e de complicações no período pós-operatório.

O desenvolvimento de métodos fiáveis para uma correta monitorização da profundidade de anestesia tem sido um dos maiores desafios da Medicina. Ao longo dos anos, vários métodos têm sido utilizados, a maioria deles baseados em avaliações visuais, resultando numa falta de objetividade.

Recentemente tem sido desenvolvido um conjunto de dispositivos para monitorização baseados na análise de sinais biológicos. Uma vez que tem sido provado que a atividade cerebral é afetada pela administração de certos fármacos durante o procedimento de anestesia geral, a grande maioria destes novos monitores baseia-se na monitorização a atividade elétrica cerebral por meio de eletroencefalogramas (EEG).

Neste tese desenvolveu-se de raíz uma metodologia baseada em tecnologias de sistemas de telecomunicações para detetar variações de frequência em sinais de EEG recolhidos de pacientes sob anestesia geral. A tecnologia baseia-se num circuito de captura de fase (do inglês Phase-Locked Loop (PLL)). Este sistema permite uma estimativa, em tempo-real, das componentes de frequência do sinal. Esta propriedade permite que não seja necessário recorrer a janelamento do sinal, durante o seu processamento, representando grandes vantages a nível da análise espetral. Deste forma, é evitado o espalhamento espetral.

Verificou-se que o circuito consegue detetar variações de frequência numa gama de ±55Hz (*Hold range*), para sinais com uma única frequência, congruente com a largura de banda dos sinais de EEG. O circuito consegue ainda seguir variações bruscas de frequência de ±20Hz (*Pull-out range*). Contudo, para sinais com várias componentes de frequência, foi observado, com o modelo Simulink, que a sincronização pelo PLL depende fortemente da frequência inicial do VCO. Devido a dificuldades de tempo não houve possibilidade de o comprovar, mas dadas as concordâncias nos restantes resultados, é de esperar que o circuito implementado consiga reproduzir os mesmos resultados do modelo Simulink.

Palavras-chave Malha de captura de fase (PLL), Monitorização de anestesia, profundidade de anestesia (DOA), Eletroencefalograma (EEG), Sincronização de frequência, circuitos analógicos.

Acronyms

AEP Auditory Evoked Potentials.

AM-DSB Double Sideband Amplitude Modulator.

AM-SSB Single Sideband Amplitude Modulator.

ANS Autonomic Nervous System.

BIS Bispectral Index.

CNS Central Nervous System.

DOA Depth of Anesthesia.

ECG Electrocardiogram.

EEG Electroencephalogram.

EMG Electromyogram.

HPF High-Pass Filter.

IC Integrated Circuit.

IFT Isolated Forearm Technique.

LEC Lower Esophageal Contractions.

LF Loop Filter.

LPF Low-Pass Filter.

MAC Minimum Alveolar Concentration.

MIR Minimum Infusion Rate.

MLAER Middle Latency Auditory Evoked Response.

MOAA/SS Modified Observer's Assessment of Alertness/Sedation Scale.

PD Phase Detector.

PFD Phase-Frequency Detector.

PLL Phase-Locked Loop.

PRST Patient Response to Surgical Stimulus.

PSI Patient State Index.

RE Response Entropy.

ROI Range of Interest.

RSA Respiratory Sinus Arrhythmia.

SE State Entropy.

SEMG Spontaneous Surface Electromyogram.

SSEP Somatosensory Evoked Potentials.

VCO Voltage-Controlled Oscillator.

VCXO Voltage-Controlled Crystal Oscillator.

VEP Visual Evoked Potentials.

VSB Vestigial Sideband.

XOR Exclusive-OR Logic.

ZXF Zero Crossing Frequency.

List of Tables

List of Figures

Contents

Chapter 1

Introduction

1.1 Historical Background

Since anesthesia was first introduced in the 19th century, there have been records of patients who recall events during surgeries, while under general anesthesia. In those days, these occurrences were caused by lack of knowledge of anesthetics' pharmacokinetics and bad practices relative to their administration.

Since then, medicine has evolved as well as our knowledge regarding drug's kinetics, neurophysiology, patient care and monitoring. A dedicated medical specialty was created focusing on linking neurophysiological processes during general anesthesia with existing patient monitoring and anesthetic techniques. The evolution of this specialty has led to a decrease in reported incidents of awareness. In the 1980s, the incidence of reports was estimated to occur in 2% of surgeries, having decreased to 0.2% as of today [1]. From these reports, approximately one third result in severe post-traumatic stress and other psychiatric disorders [2].

The increase of knowledge of pharmacokinetics and neurological processes were not the only causes for this reduction. The development of methods for anesthesia monitoring during surgeries has helped. First, subjective methods based on the observation of the patient's reaction to certain stimulations were used to assess the state of anesthesia. Even though these techniques helped the prevention of awareness, a considerable amount of incidents was still reported. More recently, with the advance of technological tools, a new branch of monitoring techniques have been developed, including a set of new subjective methods and the improvement of others. Through the monitoring of several physiological parameters, the physician decides and assesses the patient's state. Although these methods are more efficient than older techniques, they are still subject to the anesthesiologist's opinion and the surgery's conditions.

A group of objective monitors were then developed to extract several features

from physiological signals. These methods were developed to give useful information to assist the physician in his decision process. The most common and studied monitors are based on the recording and processing of the brain's electrical activity (either spontaneous or evoked). The brain's electrical activity is translated into a biosignal commonly denominated as Electroencephalogram (EEG). From the EEG processing, these monitors try to return a dimensionless number that combines a series of neurological states, parameters and events, and correlate it with the depth of anesthesia. They not only help the anesthesiologist's assess depth of anesthesia but also help in the administration of correct dosages, which leads to lower recovery times and less postoperative complications.

EEG-based anesthesia monitors resort to highly complex and advanced algorithms, extracting features and computing a single index. Most of them have proven to be able to detect, with some certainty, the state of the patient, but they have also shown to be insensitive to some anesthetic drugs, or even to return indexes that may lead the physician to take erroneous decisions [3]. Another problem associated with these monitors is that their complex algorithms lead to a delay (sometimes significant) in their response. Therefore, these devices present a past brain state of the patient. For these reasons, many clinicians have shown some hostility towards the use of these monitors, arguing that common monitoring techniques are enough and that EEG-based monitors advantages do not compensate for their complexity and costs. Others even consider that the number of incidents are too low to even compensate the investment in this systems.

1.2 Motivation

It should be pointed out that this is not a question of decreasing even more the number of incidents that in itself seems small. Few are the cases where a patient recalls any event during surgery right after his emergence. Most of these situations occur weeks, months or even years after total recovery, a period long enough to preclude any report. This suggests the probability of a higher incidence of awareness during surgery than that reported. Besides, anesthesia monitors are also used with the purpose of reducing drug dosages. It is known that high dosage of anesthetic drugs, specially during high risk surgeries (e.g. cardiothoracic procedures), often lead to postoperative complications or even death [4].

It is then a question of improving patient care by decreasing any chance of psychological damages imposed to the patients and by reducing drug dosage so as to prevent future postoperative complications.

For these reasons, now more than ever, it is necessary to take advantage of current technological developments and of the knowledge of neurophysiological processes to develop a reliable and efficient depth of anesthesia monitor.

1.3 Objectives

Neurophysiology tells us that some neurological processes exhibit specific patterns, especially those involved in consciousness and unconsciousness. These patterns are described in the EEG by several frequency components. When awake, a normal person exhibits an EEG pattern characterized by high frequency components, as a result of the brain's higher electrical activity. During the anesthetic procedure, the drugs used to immobilize and hypnotize the patient lead to a decrease in the brain's activity. This results in a change in the EEG patterns, shifting from those higher frequency components to lower ones.

In theory, there is a correlation between the state of unconsciousness and the EEG's dominant frequencies. In other words, with an increase of depth of anesthesia results a decrease in the EEG's dominant components. However, during surgery, the brain's activity should be maintained within a certain range. It should be low enough to result in unconsciousness but at the same time high enough to avoid brain damages or even death. Therefore, by tracking those frequency components it is possible to evaluate the depth of anesthesia. The proposed system should be able to detect frequency changes to higher components or lower values than those desired. Thus, alerting the physician to the dangers of the current anesthesia levels.

In this thesis, a very common and widely used circuit in telecommunications systems is considered. The mentioned technology are Phase-Locked Loops (PLL), a feedback network that has the ability to track frequency components of the input signals. The aim of this application is to take advantage of the PLL ability to efficiently track variations in frequency components of the brain's electrical activity.

Commercially available PLLs are designed to operate at telecommunications frequency bands (from kHz to a few GHz) and to deal with considerable bandwidths. EEG signals, on the other hand, consist of low frequency components and a narrow bandwidth (from 0.5 to 47Hz, approximately). Therefore, it is necessary to study the basic elements and dynamics of general PLLs and then adapt this technology to the intended application requirements.

Once this goal is achieved, the circuit must be tested, first using benchmark signals to test its performance, and then with real EEG signals collected from patients under general anesthesia.

1.4 Document Structure

This thesis focuses on anesthesia monitoring systems emphasizing on the possible application of phase-locked loops to this purpose. Therefore it is necessary to understand the background of anesthesia monitoring. First, in Chapter 2 the concept of anesthesia will be presented, exploring some of the main definitions proposed through the years. The neurophysiological processes involved during anesthesia will be addressed. Last but not least, common and available methods for anesthesia monitoring and their classification methods will be presented.

Chapter 3 will address the proposed technology and how it can be implemented as a depth of anesthesia monitor. This chapter will provide a summary regarding PLLs and their basic components. Next, an overall appreciation of the circuit dynamics will be presented, describing how can the performance be evaluated and delineating a set of parameters that define it. Since the PLL cannot use a raw EEG signal, to close this chapter the EEG preprocessing subcircuit is summarized.

On Chapter 4 the performance of the designed circuits will be extensively tested. Using software based simulations the components will be tested, first individually and then together as a whole. Matlab and Simulink tools will be used to test the preprocessing components. Then the circuit itself is tested using a SPICE-based simulator. The characteristic responses of the individual components and the complete circuit are recorded and will serve as reference for the physical implementation. After assembly, the physical circuit will be tested first with the same protocols used in the SPICE-based simulators and then with real EEG signals to evaluate the circuit's performance as an anesthesia monitor.

Chapter 5 will summarize the main conclusions and contributions of this research suggesting future work directions.

Chapter 2

Background Concepts

2.1 Anesthesia

The definition of the concept of anesthesia is still one of the problems that Medicine has failed to overcome, as well as to find an efficient and reliable method to determine its depth.

Introduced in the middle of the 19th century by Oliver Wendell Holmes [5], anesthesia was first defined as a state in which the patient is insensible to trauma during surgery. Though it continues to have the same meaning for many of us, several different opinions and definitions have originated since then in order to narrow this broad definition.

After this first attempt Woodbridge [6] proposed that general anesthesia was a result of the suppression of various nervous system's functions, resulting in events such as analgesia, hypnosis, muscle relaxation and reduced autonomic responses.

Afterwards Prys-Roberts, on the premise that pain is the conscious perception of a noxious stimulus, simplified it [7] as a state of drug-induced unconsciousness where there is neither perception nor memory of noxious stimuli. Whereas analgesia, muscle relaxation and suppression of autonomic activity were not components of anesthesia rather considered as desirable complements to this state resulting from pharmacological activity.

Whilst some consider anesthesia a complex mechanism that involves several components regarding Central Nervous System (CNS) depression, others believe that these factors must not be confused with the concept of anesthesia since they are induced by drugs. Barash [8] has recently described general anesthesia as drug-induced changes in behavior and perception to an external stimulus. Thus, the anesthetic state includes invariably components such as unconsciousness, analgesia, immobility and attenuation of autonomic response.

Despite the various hypothesis in general the idea that anesthesia results in a state of unconsciousness is shared by all of them. So the anesthetic procedure is planned in order to keep the patient unaware of the procedure and to prevent any recall.

The anesthetic procedure comprises three phases [9]: induction, maintenance and recovery. The first stage involves all the events that lead an awake patient to an unconscious stage suitable for the surgical procedure. Usually it is achieved by the administration of an high dose of drugs. Once it is reached, the anesthetic stage must be maintained to avoid any recall, thus the second stage is initiated. When the surgery is over the third phase begins, reducing the titration of drugs to allow the patient to recover its conscious state.

2.1.1 Differentiated Effects of Drugs

Ideally an anesthetic drug should induce a subject into anesthesia as fast and smooth as possible, maintaining its effect for the necessary amount of time for the progression of the surgical procedure without any adverse reaction in the patient and enabling a fast postoperative recovery. However, to the best of our knowledge, no anesthetic drug is known to combine these properties into one single substance. For this reason, current anesthetic procedures rely on a mixture of several substances to achieve the desired effect.

Usually during general anesthesia induction phase is achieved by the intravenous injection of hypnotics(e.g. propofol and thiopental) and muscle relaxants (e.g. opioids and nitrous oxide). Anesthesia maintenance is mostly accomplished through inhalation of anesthetics [10].

The commonly used anesthetic substances used are volatile anesthetics (sevoflurane, isoflurane and other halogenated ethers), nitrous oxide, opioids (e.g. morphine and remifentanil), benzodiazepines, propofol and ketamine [11].

Although the majority of these substances have similar effects in the brain's activity others show a paradoxal effect while maintaining their anesthetic activity [12]. Generally most of these drugs describe an inhibitory effect on the CNS and Autonomic Nervous System (ANS) decreasing their activity. This inhibitory activity is believed to be the reason why the patients become unconscious and are prevented from forming new memories. Perception to pain is also decreased with most of the drugs with analgesic action.

Nitrous oxide has analgesic and hypnotic effect but instead of decreasing the brain's activity it acts first as an excitatory substance preventing correct readings of the real anesthetic state via Electroencephalogram (EEG). It is not a muscle relaxant since it does not promote paralysis.

Opioids which are used for their analgesic effect have a very low hypnotic action and in over dosage conditions have antagonistic analgesic effect increasing pain sensation even if there is no noxious stimulus.

Ketamine acts as a dissociative anesthetic exciting some brain structures and inhibiting others. The problem is that the brain regions where electrical activity is recorded are those that are stimulated by ketamine resulting in erroneous readings when injected. The subject may seem conscious but it is incapable of responding.

The use of several different substances for anesthesia purposes introduced a new problem associated with the different strengths of each drug. To solve this problem two measures of strength were conceived [13]. For inhalational drugs the Minimum Alveolar Concentration (MAC) was defined as the concentration of inhaled anesthetic required to prevent 50% of the subjects from responding to noxious stimuli. For intravenous agents the analogous concept is the Minimum Infusion Rate (MIR) defined as the effective dose of anesthetic required to prevent 50% of the subjects from responding to a painful stimulation. However, nowadays both these concepts are becoming less relevant mainly because of the use of neuromuscular blocking agents which masks the action of the MAC and MIR related anesthetics.

2.2 Assessing Depth of Anesthesia (DOA)

The evaluation methods of Depth of Anesthesia (DOA) used today result from the combination of several objective and subjective methods, aiming to extract the most reliable information.

During surgery the anesthesiologist, the physician responsible for monitoring the state of anesthesia, follows a series of standard procedures to ensure the well-being of the patient through the subjective analysis of several physiological parameters. Without neglecting the presence and need of this expert throughout a medical procedure, these methods of evaluation seek to provide information as reliable and objective as possible regarding the state of the patient in order to help the physician administer the right dosage of drugs.

2.2.1 Levels of Depth of Anesthesia (DOA)

In order to quantify the state of the patient under general anesthesia during surgery one must define this state, its progression during the procedure and how it can be evaluated. By determining the components of an anesthetic state the anesthesiologist can adapt the level of drugs to the surgery timing in one hand to increase the patient's

well-being in other to decrease the postoperative recovering time and the consumption of anesthetic drugs.

In first place one needs to define the concept of depth of anesthesia (DOA). Generally and to simplify all the contrasting opinions it is defined as the probability of non-response to stimulation, weighed against the strength of the stimulus, the difficulty of suppressing the response, and the drug pharmacological effect [11]. In other words, the adequate DOA corresponds to a state maintained by the necessary amount of anesthetics to guarantee the patient's well being required by the procedure in question.

Throughout the history several models of DOA have been proposed, being all of them based on a subjective analysis of the patients' responses to noxious stimuli. The first, by John Snow, described it in five stages of narcotism [14]. The first three were related with the behavior during the phase of induction, the fourth was related to the surgical procedure and the fifth corresponded to a state of overdose where respiratory movements would become irregular or even cease.

Table 2.1: Artusio's proposal for DOA level classification based on Guedel's classification system

Artusio's Planes of Depth of Anesthesia		
Stage I	Plane 1	Absence of analgesia and amnesia
	Plane 2	Partial analgesia and total amnesia
	Plane 3	Total analgesia and amnesia
Stage II		Delirium
Stage III	Plane 1	Begin of sleep-like stage
	Plane 2	Sensory loss
	Plane 3	Loss of muscle tone
	Plane 4	Paralysis
Stage IV		Overdose (near death)

Snow's narcotism stages were then refined and generalized for other drugs by Guedel. This new scale comprehended four stages based on respiratory and ocular signs and muscle tone and was then extended by Artusio (Table 2.1) [6, 15].

Other scales based on loss of consciousness, heart rate, pain sensitivity, blood pressure and other physiological phenomenons were proposed. But as the knowledge of the brain's neurophysiology evolved, specially the processes involved during anesthesia, these classifications were proven inefficient.

Following these new studies, Griffith and Jones proposed a new classification according to stages of awareness and types of memory (Table 2.2).

More recently, with the beginning of standardized practices, two main scales were presented and have been treated as pseudo gold standard in anesthetic procedures. These are the Ramsay Scale (Table A.1) and the (Modified Observer's Assessment of

Table 2.2: Stages of the cognitive state of the patient proposed by Griffith and Jones [7]

Stage	Assessment
1	Conscious awareness with explicit recall
2	Conscious awareness with no explicit recall
3	Subconscious awareness with implicit recall
4	No awareness or recall

Alertness/Sedation Scale (MOAA/SS)) (Table A.2). Both these classification methods are based on the observation of the patients behavior and responses to several stimuli and are the basis for modern DOA classification.

2.2.2 Subjective Methods

Subjective methods rely on the movement and autonomic response to stimuli and are dependent on the physician's opinion and experience, as well as the conditions in which the procedure is carried out. With the advance of technology and knowledge of neurophysiology during anesthesia these methods become more obsolete [10, 16].

Autonomic Nervous System (ANS) response

These are the most commonly used as clinical indicators of DOA and include the evaluation of hemodynamic parameters (e.g. heart rate, oxygenation and temperature), lacrimation, sweating and pupilary dilation (mydriasis). From theses parameters a score system is implemented, the Patient Response to Surgical Stimulus (PRST). This was found to be unpredictable mainly due to the parameters not being specific to the anesthetic state. The information withdrawn is sometimes imprecise and depends on the conditions under which the procedure takes place and the anesthetic techniques applied. Furthermore it has not been proven that hemodynamic responsiveness, or the lack of it, guarantees the presence or absence of awareness [10].

Isolated Forearm Technique (IFT)

In this method a tourniquet is placed on the patient's arm before the administration of a muscle relaxant leaving the arm unparalyzed. This allows the patient to communicate during surgery when asked to move the arm. If a purposeful movement in response to a verbal command is verified then it indicates light anesthesia. Though patients have reported [10] that they heard commands but were unable to do so, which indicates consciousness but could lead the physician to assume unconsciousness. Other cases where the patient may respond to command but has no recall have been reported.

2.2.3 Objective Methods

Objective methods rely on the data acquired by highly sensitive monitors that collect several physiological signals. These monitors usually record events from muscular and brain electrical activities, heart rate and blood pressure, through Electromyogram (EMG), EEG, Electrocardiogram (ECG) and other medical apparatus. From these parameters, the monitors try to return useful regarding DOA.

Spontaneous Surface Electromyogram (SEMG)

In patients who are not completely paralyzed by muscle relaxants it is possible to record the spontaneous electrical activity of various muscle groups. It has been found that in some muscular regions, which are less affected by neuromuscular blockade, usually the muscular activity falls with increasing DOA and rises with lightning of anesthesia. But since this method is mainly dependent on the neuromuscular blocking agents it may lead to erroneous conclusions. Nowadays, this technique is used as an additional method combined with others in order to provide better overall monitoring information [10].

Lower Esophageal Contractions (LEC)

The lower portion of the esophagus is unaffected by neuromuscular blockers retaining their potential activity during surgery. From this parameter is possible to identify and study two types of movements [11], **spontaneous contractions** mediated by the ANS in which frequency decreases with an increasing dosage of anesthetic and **evoked contractions** originated as a response to the inflation of a small balloon inside the lower esophagus. Similarly to the first one, this last contraction is also affected by anesthetics where increasing dosage leads to decreasing amplitude of the movement. Due to the specificity of this technique regarding the probe's placement before the induction phase of anesthesia, the peristaltic movements of the esophagus prevent the catheter from keeping in the same position, the informations collected result in erroneous readings. Besides, as other objective methods this technique has shown a wide response variety with the type of anesthetic drug. New and more efficient monitoring techniques have made this technique obsolete [10].

ECG

During surgery the common use of electrocardiogram ECG signals is related with the monitoring and detection of cardiac events but recent studies have tried to correlate some of these events with the anesthesia procedure in order to find a new

DOA indicator. Analyzing the variability between heart beats, more specifically the periods between ECG R-wave peaks, and the difference between the heart rate during inspiration and expiration (Respiratory Sinus Arrhythmia (RSA)) it was found that this last parameter can correlate with DOA [17]. It has been reported that RSA levels reflect the level of anesthetic depth and an increase in RSA is coincident with recovery from unconsciousness [10]. Nonetheless this method has proven to fail with some common anesthetic drugs as well as a high latency (and inability to sense sudden changes of DOA)in its response.

2.2.4 Monitoring Methods based on EEG signals

Electroencephalogram (EEG) based monitors rely on the detection of the brain's electrical activity registered at the surface of the scalp. They are used to assess both the state of well-being and activity of the CNS as well as the pharmacological effect of anesthetic drugs.

An EEG signal is a highly complex, very-low amplitude and random-appearing signal. It presents no obvious repetitive patterns which makes the analysis really difficult [18]. However, some statistical studies allow the collection of some EEG characteristics that have been shown to reflect and track underlying states of the brain.

Since it has been observed that anesthesia and other mechanisms that depress consciousness are associated with increasing EEG synchrony and lower frequencies, current anesthesia monitors based on EEG signals rely on these statistical approaches to extract features through analysis in time and/or frequency domains [19].

Time Domain analysis is mainly based on the examination of the waveform's morphology over time and the extraction of statistical data such as the signal's mean, variance and power [20]. The first monitors were based on the computation of the EEG's power, and it was noted that this feature changed with the administration of some anesthetic drugs, reporting them as good DOA monitors.

Another time domain approach is the analysis of the Zero Crossing Frequency (ZXF) [9, 18] which is the estimation of an average frequency through the detection of the number of times the EEG crosses the horizontal axis (zero volts) per second. Though some correlation between a high ZXF value and patients in the awake stage and low ZXF during anesthesia has been observed, this method is very limited since it cannot translate reliable frequency information because not all components (waves) in the EEG cross the zero voltage axis and the signal is composed by multiple frequencies leading to a constant-switching ZXF value.

With appropriate training anesthesiologists can learn to recognize and extract visual features by simply observing the signal's patterns (Figure 2.1) [19]. This

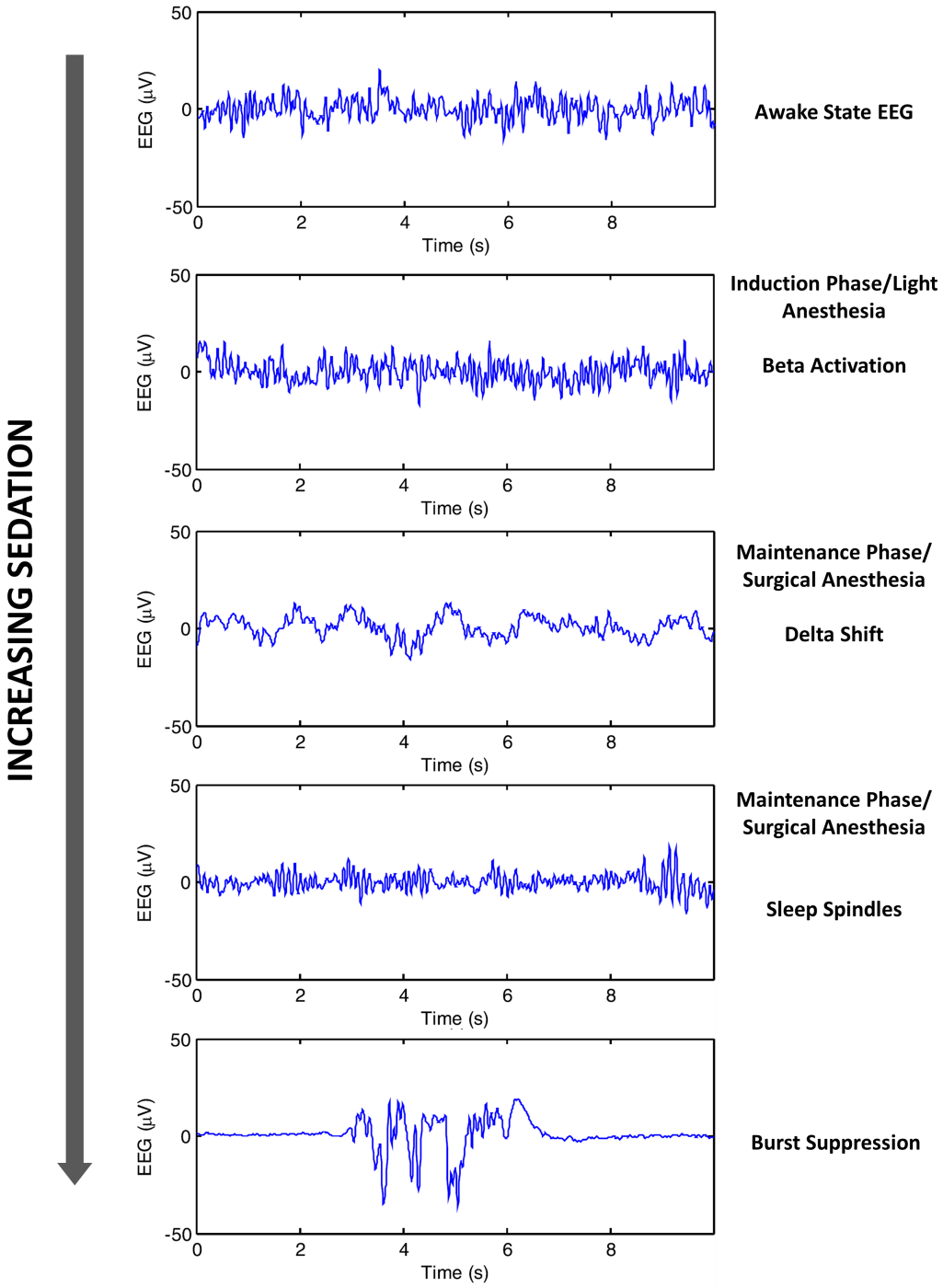

Figure 2.1: Classical EEG patterns ranging from awake state to deep anesthesia, adapted from [19]. During the awake state higher frequencies and low amplitude predominates, while with increasing sedation the signal becomes slower (lower frequencies) and with higher amplitude. The activity becomes more identical to EEG patterns observed in physiological sleep state. Sleep spindles become more evident with anesthesia deepening. Burst suppression (intermittent periods of electrical activity within an almost isoelectric line) occurs during very deep anesthesia.

skill is still particularly useful during surgery allowing the practitioners to rapidly identify specific events and act. Has one can see from Figure 2.1, during surgery the patient's EEG pattern changes drastically. Initially, the EEG is characterized by low amplitude and high frequency, when the patient is in awake state. When anesthetics are administrated (Induction Phase) the brain's activity starts to decrease resulting in an higher amplitude and lower frequency signal until unconsciousness is achieved.

During the surgical procedure, in the Maintenance Phase, it is common to observe some high frequency or amplitude episodes within the overall low frequency EEG such as sleep spindles and K-complexes related to cortical inhibition and its cognitive activity. These phenomenons are not unique to anesthesia and are present in natural sleep. This may imply the involvement of similar physiological mechanisms on both neurological stages though the levels of rousability or sensitivity to noxious stimuli are quite different [3]. Whilst in a sleep stage a person is easily aroused by a sensory stimulation under adequate anesthesia the same person will remain unresponsive to the stimulus. It is therefore important to evaluate this sensory susceptibility during surgery in order to distinguish both stages. As sedations increases brain activity falls originating an EEG close to an isoelectrical state (very low or inexistent electrical activity) alternated with brief periods of electrical activity. This state, called Burst Suppression, is common on very deep states of anesthesia but also occur with coma, hypothermia, brain injuries or even over dosage of anesthetic drugs [19].

This ability to detect specific patterns in the EEG has been used during surgery. Some developed monitors rely on this pattern recognition to help the evaluation of the anesthetic state.

More recently, **Frequency Domain** analysis has gain interest because it examines the signal as a function of frequency allowing the extraction of relevant features [21]. It is the most common analysis these days and is mostly based on the implementation of Fourier Transforms which allows the decomposition of the EEG in its fundamental components and thus attain a frequency spectrum of the signal (basically an histogram of amplitudes as a function of frequency) [18]. The basic concept behind this technique is that any arbitrarily and time-varying signal can be decomposed into simple sine waves.

Using this algorithm was possible to identify specific EEG patterns correlated to brain activity and discriminate them into specific frequency bands. Classically the brain's electrical activity is divided into five frequency bands (Table 2.3).

An awake and normal person presents a brain activity mostly within beta[1] (β) band, with a pattern dominated by high frequencies. During anesthesia sedative drugs change the dominance of these frequencies leading to a shift of the signal's power into

other frequency bands, first to theta (θ) and at deep anesthesia to delta (δ) band. If DOA increases electrical activity decreases to a Burst Suppression state or even to dangerous isoelectricity.

Table 2.3: Classical EEG Frequency Band distribution.

Frequency Band Designation	Range (Hz)
Delta (δ)	0.5 - 3.5
Theta (θ)	3.5 - 7
Alpha (α)	7 - 13
Beta (β)	13 - 30
Gamma (γ)	30 - 47[1]

Nowadays there are several monitors of DOA based on the analysis of the brain's electrical activity during surgery, most of them try to rate the brains activity state into an index for easy classification. Though with some limitations (e.g. have insensitivity to some commonly used anesthetic drugs) they have received special attention and have entered the surgical environments as a new anesthesiologist's helper. Yet reference must be made regarding these monitors properties. They are monitors of the brain state not of drug levels and caution must be taken if called as predictors since they present, due to latency, a past state of the brain that may be different from the current state.

The most common monitor is the Bispectral Index (BIS) monitor. Nevertheless, other monitors exist and are examined below.

Bispectral Index monitor (BIS)

The Bispectral index monitor (Aspect Medical Systems Inc., Natick, Massachusetts, USA) is the most studied and used anesthesia monitor based on EEG analysis in surgical environments and is characterized by the implementation of a bispectral analysis. It returns an index between 0 (no electrical activity) and 100 (awake) and ideally should be kept between 45 and 60 during surgery [23].

Bispectrum is a third order statistical measurement of the correlation of phase between different frequency components. Though it is not known the physiological significance of these phase relationships bispectrum analysis has several advantages concerning EEG processing, such as, noise suppression and identification of non-linearities [18]. Bispectral analysis examines the relationship between two primary

[1]There have been some disagreement related to the EEG's frequency band boundaries. Because the EEG is recorded in the scalp it acquires noise specially at higher frequencies. Studies have shown that frequencies above 20Hz are contaminated with EMG signal [22] though others have shown that the gamma frequency band is important in the evaluation of DOA [3]. In this work, the 47Hz frequency will be considered the higher boundary of the EEG since it is the same frequency used in most anesthesia monitors.

frequencies and the phase information is returned by bicoherence (a measure of phase coupling between both frequency components). A strong phase coupling implies that the components have a common source. This may provide information of the interaction between different brain structures.

At the end the BIS is a dimensionless number computed using time and frequency domain features extracted from EEG signals as well as data extracted from EMG and ECG signals. The parameters [24] were derived and quantified from a collected database of EEG signals and correlated with several sedation scales mentioned in Section 2.2.1 (Tables A.2 and A.1). From these parameters three are the most relevant:

Burst Suppression Ratio a time domain parameter that reports the fraction of time that the EEG is suppressed (near isoelectrical)

Beta Ratio a frequency domain parameter relative to the logarithmic ratio between the power of two frequency bands 30-47 Hz and 11-20 Hz.

SynchFastSlow a parameter retrieved from the bispectral analysis related to the logarithmic ratio of the sum of bispectrum peaks within the band 0.5-47 Hz over the sum of the total bispectrum within the range 40-47 Hz. Each parameter was chosen to correspond their sensibility to a specific anesthetic effect. The algorithm used weights and combines these parameters in order to quantify and determine the state of the brain during anesthesia. Beta Ratio predominates when the EEG has light anesthesia characteristics while SynchFastSlow is more dominant during hypnosis and burst suppression ratio detects deep anesthesia.

The BIS monitor has proven reliable [3, 23–26] both in determining the patient's state of anesthesia and reducing the use of drugs during surgery. However, studies have shown this monitor is not useful when some substances are used (e.g. nitrous oxide, ketamine and opioids). Although the manufacturer indicates that the index should be maintained between 45 and 60 to ensure unconsciousness several studies have present cases of awareness during the procedure even when BIS values were kept within the suggested range [3].

Narcotrend

The Narcotrend *(MonitorTechnik, Bad Bramstedt, Germany)* monitor uses an algorithm based on pattern recognition of raw EEG and classifies them into five stages form A (awake) to F (burst suppression and near isoelectrical) returning also a dimensionless number between 0 (electrical silence) and 100 (awake) [25].

A pattern recognition software evaluates the patterns described in Figure 2.1 and uses features extracted from both time and frequency domains. The software is trained

using a database of previously classified features using characteristic EEG signals from sleep stages [27].

Although some studies have claimed the clinical application of the Narcotrend as DOA monitor, others have found that this device is not as reliable as others in determining with confidence the real state of DOA. In addition to the device's insensitivity to some anesthetic drugs, specially neuromuscular blocking agents it shows a great delay in its response comparing with other monitors [28] .

M-Entropy

Common EEG-based monitors rely their quantification of anesthetic drugs effects on frequency domain analysis. Since it is evident that the brain's electrical activity changes with sedation and loss of consciousness this approach has proven reliable. Furthermore, those ever changing electrical patterns show that neuronal systems present nonlinear and chaotic behavior. One method that deals with this kind of dynamic systems is entropy, a concept theorized in thermodynamics to describe the state of gaseous and fluid systems. Entropy was adapted to measure the information within a given amount of a signal in order to describe its complexity and unpredictability.

Using entropy to achieve predictable future amplitude values of the glseeg, based on probability distribution of the already observed amplitude values, it was found that these distributions (which are basically probability density functions) change in appearance with different anesthetic states [29]. There is a commercial device based on this theory to evaluate the DOA on surgical environments called M-Entropy (GE Healthcare Finland, Helsinki, Finland) [25]. The M-Entropy uses an algorithm that estimates two different entropy variables through the application of Fourier Transform to the EEG signal: State Entropy (SE) and Response Entropy (RE).

The first parameter (SE) is a measure of the disorder of electrical activity within the frequency range of 0.8 - 32 Hz, reflecting the hypnotic state of the patient. The second variable (RE) measures both EEG and EMG activity in the frequency range of 0.8 - 47 Hz. By including facial muscle activity this monitor may become sensitive to neuromuscular blocking agents action [30]. Normalizing both variables enables the evaluation of both consciousness (from SE) and state of analgesia (using RE). If RE is equal to SE then there is no evident muscular activity which may be translated into an adequate analgesia.

The M-Entropy monitor returns an index between 0 (suppressed EEG) and 100 (awake with evident muscular activity). It has proven reliable with common anesthetics reducing the incidence of unwanted events such as hypertension but in the presence of other anesthetic drugs (e.g opioids, ketamine and nitrous oxide) has

shown contradictory results leading to underestimation of DOA [29]. Nonetheless it has a better performance in detecting consciousness comparatively to other monitors. Furthermore, it has led to decreasing titration of anesthetics during the procedure, though it has not been proven any advantage concerning faster postoperative recovery times [31].

Patient State Index (PSI)

The Patient State Index (PSI) monitor returns a dimensionless number between 0 (no electrical activity) and 100 (awake) that classifies the DOA state according to the MOAA/SS [32].

From the assumption that during loss of consciousness posterior and anterior portions of the brain become detached and that specific brain structures have different activities during consciousness or unconsciousness [33], the PSI uses an algorithm that incorporates several quantitative EEG parameters that reflect brain activity. These features include changes in power in various EEG frequency bands, changes in symmetry and synchronization between brain regions and inhibition/activation of regions of the frontal cortex. From theses parameters the algorithm computes temporal and spacial gradients that describe changes in electrical activity between several brain structures [34].

The commercial monitor based in this technology is the SEDLine (Masimo Corp., Irvine, California, USA) and it has been frequently studied and validated in comparison to the BIS monitor [32–36]. As all other monitors it shows a good performance detecting DOA with common anesthetics, allowing the reduction of the use of several drugs and faster recovery from anesthesia. Compared to the BIS monitor it performs as good as the widely used monitor. The PSI monitor is not as fast detecting changes in brain activity as the latter but makes better use of the predefined index range resulting in a more pondered use of anesthetics.

Evoked Potentials

Another approach distinct from the monitoring of spontaneous brain activity is by observing the changes in the brain's activity caused by specific external stimuli. These changes are called Evoked Potentials and their recording through EEG allows a more localized monitoring of the brain's activity [10]. This method allows the quantization of the EEG by measuring post stimulus latency and waveform amplitudes. The latency reflects the time required for the neuronal information to be transmitted to successive brain structures. As long as a subject maintains in a stable state the latencies remain stable. Therefore, changes in propagation velocity of the evoked potentials caused

by anesthetics can potentially provide an indicator of the rousability of a given brain structure [37].

On a surgical environment three types of evoked potentials ate commonly used based on the sensory stimulus:

Somatosensory Evoked Potentials (SSEP) are changes recorded on the somatosensory cortex in response to tibia, peronial or median nerve stimulation.

Auditory Evoked Potentials (AEP) are the changes recorded at the primary auditory cortex in response to auditory stimulation. These are the most common for the assessment of anesthetic drug effect. These potentials can be divided into several domains as function of latency being the most studied the Middle Latency Auditory Evoked Response (MLAER) that extends from 6 to 60ms after stimulation.

Visual Evoked Potentials (VEP) are recorded at the primary visual cortex in response to optic stimulation.

Evoked potentials components have proven to change during anesthesia procedures [38]. Whilst some anesthetic drugs (e.g. intravenous drugs)tend to increase AEP latencies others (e.g. inhalational anesthetics) change these potentials' amplitude. In fact this technique is the only method sensitive to DOA changes when the surgical procedures uses nitrous oxide and opioids as sedation agents. Conducted studies evidenced the effectiveness of AEP as an indicator of DOA allowing a more sensitive and robust tracking of the anesthetic state in surgical environments delivering the best performance in distinguishing the transition from unconsciousness to consciousness [37].

A DOA monitor is supplied by Alaris AEP Monitor (Danmeter Inc., Odense. Denmark) which is based on the analysis of the MLAER to compute a new index related to DOA called Auditory Index [39].

Even though the benefits that evoked potentials technique have brought it involves some technical and clinical complexities regarding signal recording, acquisition and its processing.

All of the presented methods and monitors have been thoroughly studied and validated as DOA assessment techniques. As knowledge on neurophysiology increases and technology evolves objective methods of assessment present better results making subjective methods more and more obsolete. Nonetheless, these monitors are based on numerical algorithms applied to digitized signals. If the analysis of a single frequency signal is as simple and easy as it can be, extracting features of a signal as complex as an EEG not so much. Therefore, these technologies will maintain a certain amount of flaws mostly because of their complex algorithms with high computation requirements,

signal's characteristics and also limitations of numerical algorithms.

A new approach is proposed in this thesis and is based on the implementation of telecommunication technologies to track and interpret the information within the EEG signal recorded from surgical procedures. It is expected that the proposed approach should be able to evaluate the state of anesthesia during surgery. This method is based on the implementation of a Phase-Locked Loop (PLL), a quite simple and common circuit on telecommunication systems.

Chapter 3

Designed System Concepts

An EEG signal describes the complex electrical activity of the brain. Because of its characteristics the analysis of this signal is highly challenging and unique. In telecommunication systems it is common to find complex signals even though their composition is simpler than the EEG's and operate at quite different frequencies. Nonetheless, is somehow logical to adapt some telecommunication technologies to EEG signal processing [40–43].

One technology that has always aroused interest for its simplicity and efficient operation is the Phase-Locked Loop (PLL).

In this Chapter, PLL fundamentals and its circuitry design will be explored in order to understand how it can be exploited leading to a system able to assess the frequency content of an EEG and consequently acting as a monitor for anesthesia-related applications. The basic structure of the PLL will be analyzed from an electronic point-of-view, presenting some of the most common solutions and how can they be implemented. A study of the complete loop will be made to understand how the chosen components interact with each other and how they influence the loop dynamics.

Furthermore, and since the PLL can not operate by itself, the acquisition and preprocessing of the EEG signals will be addressed examining how they can be used as an input signal to the PLL.

Finally, to close the chapter, the final design of the loop that will be implemented and tested as an EEG tracking device will be presented.

3.1 Phase-Locked Loops (PLL)

A Phase-Locked Loop (PLL) is a common circuit with several applications in the area of communications [44]. It consists in a feedback control loop with three main

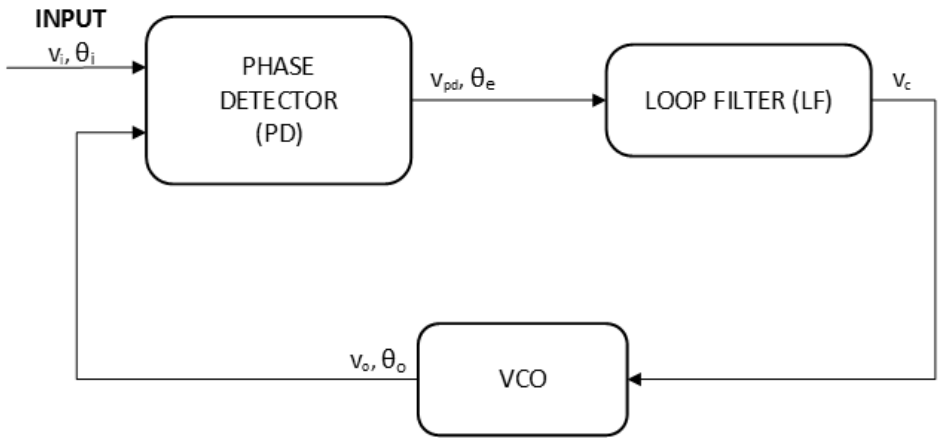

Figure 3.1: Basic PLL block schematics

components, a Phase Detector (PD), a Loop Filter (LF) and a Voltage-Controlled Oscillator (VCO) (Figure 3.1). It can be found in modulators, demodulators, frequency synthesizers, multiplexers and other signal processing applications [45]. PLLs have interesting properties that make their broad use in telecommunications, as the ability to automatically track periodic signals and extract their instantaneous angle (frequency and phase) under severe noise conditions.

The PLL operation is quite simple. The PD compares the phase of the input signal with the phase of the VCO output resulting in a phase error. The error signal is then fed into the filter (essentially a low-pass filter) producing a voltage to act as control to the VCO. The oscillator is then forced to vary its frequency with the aim to minimize the phase difference between the VCO output and the input signal. When the phases are sufficiently close, the loop attains the lock state, and the VCO remains synchronized with the input. As a consequence both frequencies should be equal in lock conditions [45, 46].

Hence, the loop must be able to track the desired components of the input signal. This requires the loop to be resistant to the presence of noise and have the required celerity for the application. These properties depend on the loop's bandwidth. A narrow bandwidth is suitable for applications that involve input signals embedded in noise where the PLL can be used to recover either the signal or its properties thus removing the noise. However, it makes the loop slow on tracking the main frequency component limiting its application to fast and non-stationary signals. On the other hand, a wide bandwidth gives the loop a fast response to signal changes but more sensitive to noise [47].

For these reasons, a PLL circuit operates best at higher frequencies since it allows the loop o have a narrower bandwidth but with a higher tracking speed. At lower

frequencies the loop has a poor performance [46].

The loop's linearity is another property that one must take into account. A PLL consists in nonlinear components thus resulting in an overall nonlinear loop [48]. Although, some PLLs can be analyzed using linear techniques under lock conditions.

Its ability to extract time-varying frequency information associated to its resilience to noise makes it suitable to EEG signal processing, more specifically to track its main frequency components. Furthermore, being an analog circuit results in the development of a real-time system that monitors the EEG's rhythmic activity [43].

Next the individual components of the PLL will be examined, presenting some of the most common solutions and those that will be tested to implement in the final device.

3.1.1 Phase Detector (PD)

The Phase Detector (PD) is a component capable of producing a voltage signal proportional to the difference between the phase of the input signal (θ_i) and the phase of the VCO output (θ_o) producing an error signal with a specific phase (called phase error θ_e). So in ideal conditions the phase error can be defined as [45]

$$\theta_e = \theta_i - \theta_o \tag{3.1}$$

Although in real conditions other factors must be taken into account. When the input signal is null the PD generates a residual voltage, called free-running voltage (V_{do}). In addition, each type of PD has its own and specific gain (K_d).

Hence, the PD output signal (v_{pd}) can be modeled by [48]

$$v_{pd} = K_d\theta_e + V_{do} \tag{3.2}$$

This linear model fails for large phase errors. The values of θ_e for which the linear model is valid are called the range of the PD.

Two main classes of PD can be pointed out: multiplier circuits and sequential devices. While an analog multiplier generates the phase error as the product of the input signal waveform with the VCO waveform, sequential PD generates a useful error-output that depend solely on the time interval between a transition of the input signal and a transition of the VCO waveform [49].

Analog Multipliers

These were the first kind of PD used in PLL design and are one of simplest components. They have good performance specially when used in the design of linear PLLs. A properly designed multiplier is able to operate with signals deeply embedded in noise [50].

When both inputs are sinusoidal the output signal can be described by [51]

$$v_{pd} = A_1 \sin(w_i t + \theta_1) \cdot A_2 \cos(w_i t + \theta_2) = 0.5 K_m A_1 A_2 \sin(\theta_e) + 0.5 K_m A_1 A_2 \sin(2 w_i t - \theta_e) \tag{3.3}$$

Where K_m is the multiplier's gain, the first term is the linear component of interest and the second term a high frequency component which can be attenuated by the loop filter. Usually this component is higher than the filter's cutoff frequency so it doesn't influence the PLL's locking performance [46].

The most common PDs of these kind are four-quadrant multipliers, like the Gilbert cell (Figure 3.2(a)), and Diode Mixers (Figure 3.2(b)) [45].

Gilbert Cell The Gilbert cell is one of the most common and studied analog multiplier. It is composed by active elements and can be assembled in many architectures being the most common the four-quadrant multiplier (it allows both input signals to have positive and negative amplitudes) [52]. The Gilbert cell PD has a well-known PD gain that can be easily adapted through the resistors in the circuit and the bias current (I_{ee} in Figure 3.2(a)). However, requires both resistors and transistors to be exactly matched. A mismatch between these components can cause voltage offsets [53].

This circuit can withstand several input waveforms (e.g. sinusoid, square and triangular waves). Though it performs best with sinusoidal waves [45]. Furthermore, the input signals must be kept within the linear region of the transistors, and the output amplitude signal results from the product between both input amplitudes (A_i and A_o) with the multiplier's gain K_m [47]

$$v_{pd} = K_d sin(\theta_e) = 0.5 K_m A_i A_o sin\theta_e \tag{3.4}$$

Ideally the Gilbert cell output (after removal of the higher frequency components) v_{pd} should be described by Equation (3.4). One can denote that PD gain K_d is not a property of the circuit alone depending also on the input signals.

Although it's an efficient circuit, the Gilbert multiplier has the disadvantage of using active elements, which increases the system's power consumption. Also, it as a

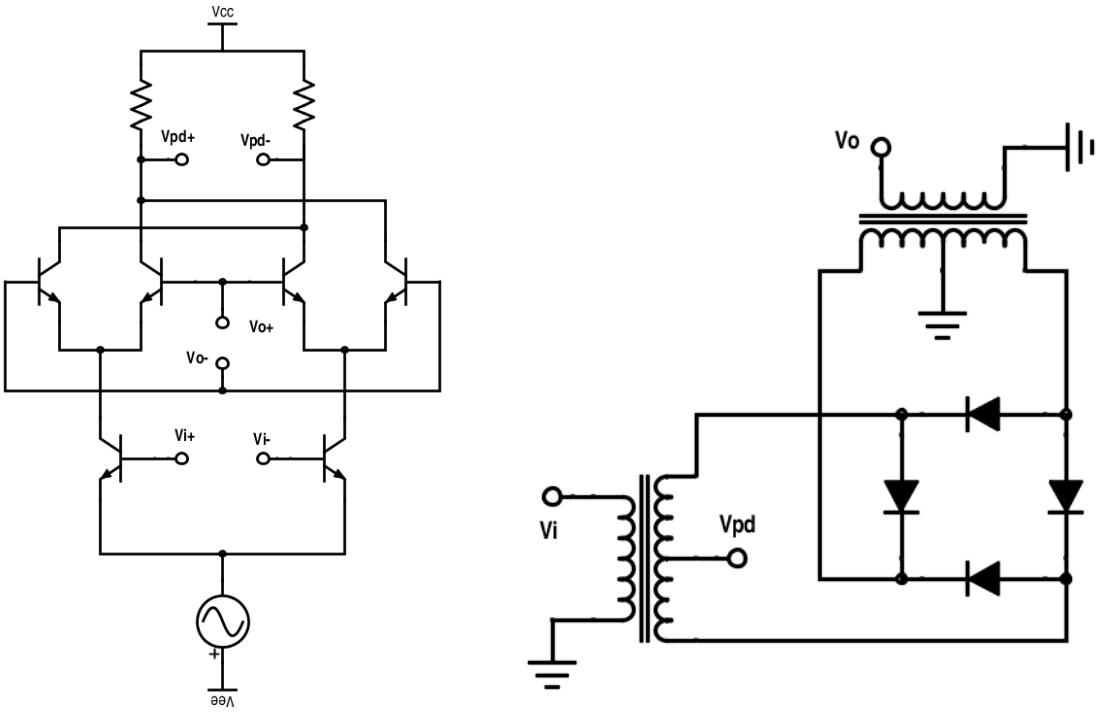

(a) Gilbert multiplier (b) Diode ring mixer

Figure 3.2: Examples of common analog multipliers, adapted from [46]

more limited bandwidth because of the transistors and requires care with impedance balance between the PD circuit and the external components.

Diode Ring Mixer Another simple and common circuit are the diode mixers. They are tolerant to a wide range of operating conditions and show properties identical to analog multipliers. The diode mixer can operate with all kinds of signal waveforms and at higher frequencies than transistor-based multipliers [47]. Besides, it is uniquely composed by passive components imposing a small burden to the PLL designer and the circuit itself.

However, to operate as a PD one of the input signals (v_i) must be much smaller than the other (v_o), to prevent the diodes from conducting, and usual output amplitude values are between 0.3 and 0.4 V (volts) [46].

For these conditions and considering that the transformers have a number of primary turns equal to the number of secondary turns, then the PD gain depends solely on the amplitude of v_i (i.e. A_i). The gain of this circuit can be determined by [46]

$$K_d = A_i/\pi \tag{3.5}$$

Nonetheless, these conditions are often violated in practical conditions, which makes this analysis an approximation.

Sequential Phase Detectors

This type of PD operates through the detection of transitions of the input signal waveforms, making it insensitive to other properties as the type of waveform and amplitude. Usually sequential PDs operate best with square waves but can also operate with other waveforms [45–47]. These circuits make use of logic components to detect signal transitions.

Sequential PDs have a linear region of operation for a certain range of phase error values. Each type of PD has its own characteristic region [47], although the transfer function in the linear region is the same for every sequential detector, given by:

$$v_{pd} = K_d \theta_e \tag{3.6}$$

There are several architectures that can be used as sequential PDs, the most common are Flip-Flop circuits, Exclusive-OR Logic (XOR) circuits and the Phase-Frequency Detector (PFD).

Exclusive-OR Detector The XOR operates similarly to analog multiplier circuit under saturation conditions (overdriven). When overdriven, the multiplier outputs a positive voltage if both inputs are simultaneously positive or negative. If one of the inputs is positive and the other is negative then the output will be negative [45]. In logic circuits the first case results in a 'high' level output and the latter in a 'low' level state.

As logic circuits have active components, they are supplied by a voltage V_{cc}, so a high-level corresponds to an output saturated in V_{cc} and a low-level to an output at ground (zero volts).

Using XOR as PD has the advantage of the attainment of fixed and higher PD gains (K_d) and less offset voltages [46]. The gain depends only on the voltage supply (V_{cc}) and on the component's range

$$K_d = \frac{V_{cc}}{\pi} \tag{3.7}$$

Ideally the XOR has a linear transfer function when phase error is within the range 0-π radians (rads) [47].

The XOR bandwidth is defined by the loop filter characteristics allowing for a

high capability of retaining lock even with very noisy input signals. Nonetheless, the logic circuit presents some nonlinearities that can aggravate the effect of noise in some conditions. Another disadvantage is that this PD is sensitive to the input signals duty cycle[2] [47].

Flip-Flop The most simple Flip-Flop based PD is the RS Flip Flop. This kind of logic circuit has an increased linear range of operation, compared to the XOR PD, ($\pm\pi$ rads) and is not sensitive to the signals' duty cycle. However for the same supply voltage has a lower PD gain [45]

$$K_d = \frac{V_{cc}}{2\pi} \tag{3.8}$$

Furthermore, the RS Flip-Flop has de disadvantage of being more sensitive to noise present in the input signals [47].

Phase-Frequency Detectors (PFD) This is widely used and studied sequential PD. It is a logic component like the previous two but it presents a more complex operation [46, 54, 55]. It has a linear range of $\pm 2\pi$ radians and act as both phase and frequency detector. Therefore, when both input frequencies are initially different (out of lock state) it gives a better performance to the loop in reaching lock state [46]. It is not sensitive to the signals duty-cycle Because of its wider range it has a lower K_d gain [47]

$$K_d = \frac{V_{cc}}{4\pi} \tag{3.9}$$

For the desired application and the characteristics of the EEG signal an analog PDs would be more suitable since they can operate with several types of waveforms. However, sequential PD's, specially the PFD, allow for a better noise and lock performances [55]. Considering these characteristics, a wide linear phase range and its insensibility to signals' duty-cycle then the PFD was selected. Yet, a problem regarding the need of a square-wave input arises. This problem and how to solve it will be addressed later on.

3.1.2 Voltage Controlled Oscillator (VCO)

This is the heart of the PLL. This component is responsible for the PLL's oscillatory response and outputs a signal with a frequency dependent on the input voltage.

[2]Duty cycle of an high and low level signal (or square wave) is the ratio between the duration of the high level and the low level, during a full period of the signal

The circuit is sometimes called a voltage-to-frequency converter because the output frequency is tuned by the input voltage.

During the design of the oscillator some requirements are desired [45], usually a compromise must be achieved between the following characteristics: low phase noise, frequency accuracy, wide tuning range, tuning linearity, fast response, low power consumption and immunity to external noise/influences.

Linearity is one of the most important property that a VCO should present. Ideally the VCO's frequency ω_o should be a linear function of the control voltage v_c (output voltage of the loop filter), and given by [46]:

$$\omega_o = K_o(v_c - V_{co}) + \omega_i, \tag{3.10}$$

where K_o is the VCO's gain, ω_i is the PLL's default frequency and V_{co} the value of v_c for which $\omega_o = \omega_i$.

There are several solutions that can be used as VCO [45]. The two most common types are relaxation and resonant oscillators. Each has advantages and disadvantages in terms of the desired properties.

Relaxation Oscillators

A relaxation oscillator is a circuit that repeatedly alternates between two states with a period that depends on the charging of a capacitor [56]. One of the most common relaxation oscillator is the 555 timer in astable mode (Figure 3.3). The 555 is a popular timer for several applications due to its various operation modes [57]. In monostable mode, the 555 produces a precise frequency square wave, but for VCO application, the 555 must be programmed to operate in astable mode as shown. The astable mode allows the timer to generate a square wave output with a voltage-controlled frequency.

The astable mode is achieved by forcing the 555 timer to re-trigger itself. If both inputs pins 2 (Trigger) and 6 (Threshold) are connected to each other, re-triggering will happen causing a continuous charging and discharging of the capacitor C1 [57]. So it's the charging and discharging times that define the astable's frequency of oscillation, and therefore the 'high' and 'low' periods of the output wave.

The charging and discharging times, t_1 and t_2, respectively, are defined by [59]

$$t_1 = (R_1 + R_2)C_1 \ln(2) \tag{3.11}$$

$$t_2 = R_2 C_1 \ln(2) \tag{3.12}$$

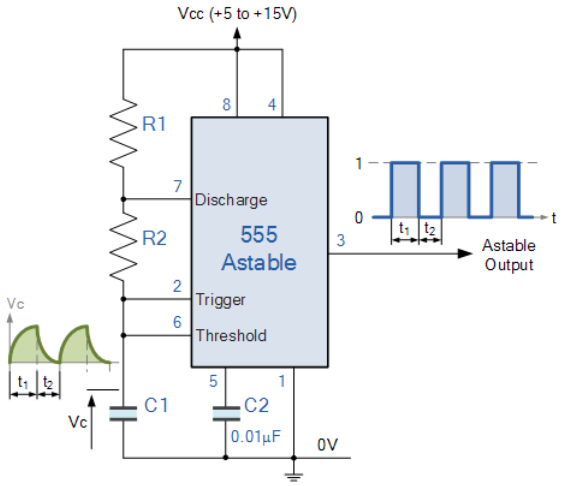

Figure 3.3: 555 timer in astable mode [58]

Then the period T of oscillation is defined by the sum of charging and discharging times [59]

$$T = t_1 + t_2 = (R_1 + 2R_2)C_1 \ln(2) \tag{3.13}$$

Frequency of oscillation f_o can be obtained by the following relation [60]

$$f_o = \frac{1}{T} \tag{3.14}$$

It is possible to use the Control input pin (pin 5 in Figure 3.3) of the 555 timer to control the capacitor's charging/discharging cycles and therefore change the frequency of oscillation [57]. The input Control voltage v_c changes the threshold values of the internal comparator of the 555 leading to a change in charging/discharging periods. And so the period of oscillation T_o is defined by [59]

$$T_o = t_1 + t_2 = (R_1 + R_2)C_1 \ln\left(\frac{V_{cc} - v_c/2}{V_{cc} - v_c}\right) + R_2 C_1 \ln(2) \tag{3.15}$$

where v_c is the input voltage, when the capacitor C2 of the Figure 3.3 is replaced by a control voltage on pin 5.

From Equation (3.15), one can conclude that the frequency is not directly proportional to the input control voltage. Although, since the 555 astable VCO as a high bandwidth it is possible to delimit a smaller bandwidth where a frequency-voltage relation may be considered linear.

Another advantage of a 555-based VCO is its low power consumption and can easily be mounted in an Integrated Circuit (IC) [61]. Though they are more susceptible to

external and internal noise sources and to temperature. Relaxation oscillators usually present a lower VCO gain constant than resonant oscillators [56].

Another problem related to this circuit is its duty cycle. Preferably the astable circuit should output a near 50% duty cycle signal. This can be attained but only for a very small bandwidth. For most of the VCO's frequency range the output square wave exhibits a quite variable duty cycle [57]. Caution must be taken when using a 555-astable as the VCO for the PLL circuit. As seen before, there are PDs sensitive to the input's duty cycle so the designer must be careful when choosing the appropriate PD.

Nonetheless, this kind of VCO seems to be adequate for a EEG tracking system. The astable oscillator allows for a wide bandwidth and a fine control of frequency. It presents good frequency stability and better performance at low frequencies and has an acceptable stability under noisy signals [45]. An imposed concern is the output's variable duty-cycle of this type of oscillator that will affect the choice of PD.

Resonant Oscillators

Resonant oscillators are another common type of oscillators used in VCO applications, the most common are LC Oscillators and Crystal Oscillators [62].

LC Oscillator Another possible solution to develop a VCO is by using a LC oscillator. This oscillator is based on a network of inductances (L) and capacitances (C) that oscillates through the supply of a certain voltage. The circuit's frequency of oscillation ω_o is given by [63]

$$\omega_o = \frac{1}{\sqrt{LC}} \tag{3.16}$$

Introducing a variable capacitance (given by a varactor) the frequency ω_o may be controlled.

Most semiconducting components, like diodes and transistors, have shown a variable capacitance depending on their polarization. Whilst most diodes are designed to minimize this effect, a varactor (variable capacitance diode) is developed to take advantage of this property [64]. The varactor operates in reverse-biased state where the thickness of the depletion zone varies with the control voltage (v_c). This causes a variation to the varactor internal capacitance. Combining this property to a LC circuit, it is possible to develop a LC-VCO, as shown on Figure 6-b).

The varactors have very low capacitances (in the order of picofarads), which make the LC-VCO suitable for high frequency applications.

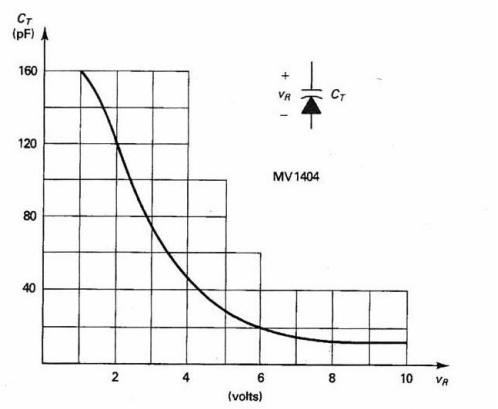

(a) Varactor characteristic

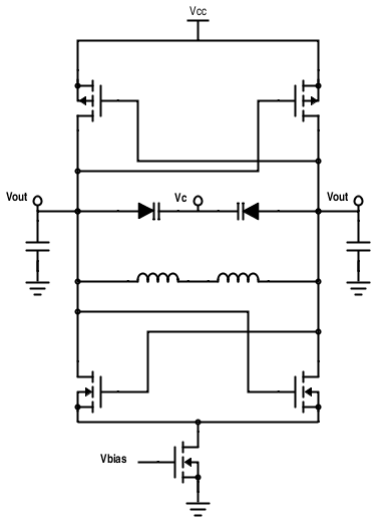

(b) LC VCO circuit example with varactors

Figure 3.4: LC-VCO basics [47]

This type of VCO have an improved resistance to noise, stray signals and temperature compared to Relaxant Oscillators [63]. Being essentially a LC resonator the circuit's properties can be evaluated through its Q factor (or quality factor) which can be calculated by [60]

$$Q = \frac{r_p}{\omega_o L}, \tag{3.17}$$

where r_p is the equivalent impedance of the circuit, L its inductance and ω_o the resonant frequency. The higher the quality factor the better is the VCO performance (e.g. higher frequency stability and higher immunity to noise) [63].

To adapt a LC-VCO to the required low frequencies in this thesis a very high inductance and capacitances would be required which may be hard to attain in practical applications. Besides being impractical it would reduce drastically the Q factor, reducing the output's frequency precision and noise immunity. This oscillator lacks linear behavior and have a bad fine tuning, meaning that a small and linear change in the capacitance is hard to obtain, for a wide range of control voltage [65].

Crystal Voltage Controlled Oscillators (VCXO) This architecture is ideal for applications that require a PLL with extremely low bandwidth without decreasing the VCO's gain [46].

Using a crystal oscillator as the basis of the circuit presents great advantages: high levels of frequency stability and low levels of phase noise can be maintained

while still being able to control the frequency over a small range [47]. To design a Voltage-Controlled Crystal Oscillator (VCXO) one can simply use a standard crystal oscillator which uses a piezoelectric element to generate a precise frequency signal built in an electronic support circuitry. This circuit must be able to slightly tune the crystal's frequency. The amount by which the frequency can be pulled depends upon a variety of factors, but usually is accomplished by applying a variable capacitance. Caution must be taken because for wider frequencies may be required the use of higher capacitance changes (difficult to achieve) or introduction of inductances in the circuit [46].

The VCXO has a high quality factor Q which is the reason for its stability, however, the fact that one is able to vary the frequency of oscillation reduces the Q value [46]. The wider is the range of frequency change the poorer will be the circuit's stability.

Another problem is its sensitivity to temperature. Crystal oscillators have a good temperature stability but once again when their frequency is tunned this property is lost, and sometimes the temperature drift can be considerable [56].

VCXO have remarkable advantages, if the application requires high frequency operation over a small range of frequencies. This is why this component is usually implemented when the PLL operates as frequency synthesizer [47]. For wider frequency ranges a compromise must be attained between frequency, noise and temperature stability. For this thesis, a VCXO is not that suitable because the system will operate at very low frequencies.

After a deep analysis of the advantages and disadvantages of all possible VCO architectures and weighing them with the final application, we realize that the 555-astable oscillator represents the best compromise between low frequency performance and noise sensitivity.

3.1.3 Loop Filter

The phase detector's output v_{pd} consists in various components one of them proportional to the phase error θ_e and the others containing high frequency elements. The latter are undesired so a filter can be introduced in the loop to remove them and output the phase error component close to a DC component [45]. Therefore, the loop filter is essentially a Low-Pass Filter (LPF).

The filter can be a simple element, so one can either use a basic RC filter using only passive elements or an active filter for better overall performance. The type of filter must be taken into consideration. The filter is responsible for the modulation of the overall dynamics and for the restriction of the PLL's frequency range and locking

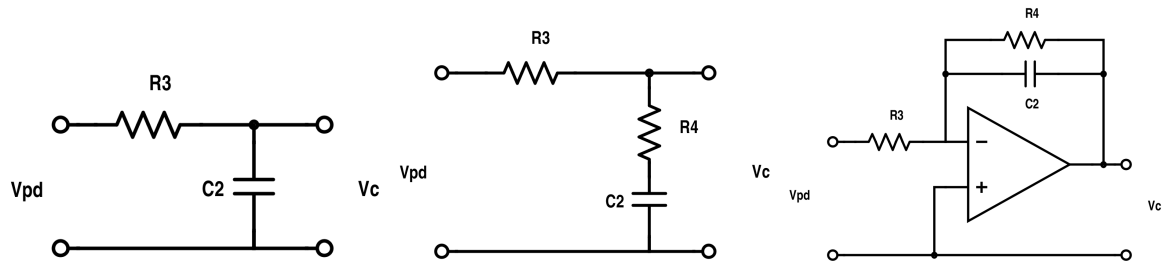

(a) Simple passive low-pass filter (b) Passive Lag-lead filter (c) Active low-pass filter

Figure 3.5: Common loop filter architectures, adapted from [60]

speed [48].

A first order passive filter is usually enough for most applications, allowing low power consumption and simple circuitry. The first choice would be to use a simple LPF like the one shown on Figure 3.5(a). In theory it would suffice, as it does in some practical applications. However, it is preferable to add a resistor in series with the capacitor (Figure 3.5(b)) to add more stability to the filter, although sacrificing bandwidth. This extra resistor adds a pole to the loop filter transfer function (see Section 3.1.4). The absence of this pole would make the loop highly sensitive to any slight disturbance leading the PLL to unstable states [45].

Passive filters have the advantage of linear operation with low noise and can be used for any frequency range (virtually have unlimited bandwidth) [46]. However for high values of resistance and capacitance they are harder to integrate in the circuit.

An active filter (Figure 3.5(c)) on the other hand can provide a fast locking response to the loop maintaining the dynamic properties of the loop. It allows also the addition of an extra gain K_f to the loop's transfer function. It can also reduce the passive components values using transresistance architecture [66]. Nonetheless, the high gain makes it more sensitive to noise and the use of an operational amplifier (op-amp) reduces the loops bandwidth. It also increases the power consumption of the overall circuit [67].

Higher order filters can be used to achieve better performances. They allow a faster frequency response and steeper rolloff in order to suppress higher frequency disturbances (e.g. noises) [60]. Though high order loops have a more difficult analysis.

For the intended application (an EEG frequency tracking monitor) since the signal has a very low frequency (maximum frequency considered will be 47 Hz) and a relatively small bandwidth (frequency range between 1-47Hz), when the input signal is baseband, and given the desired loop dynamics (will be discussed latter on) the use of a first order active filter like the one described in Figure 3.5(c) seems the most appropriate solution.

The name loop filter may be misleading. It is designated so because most PLLs use a LPF as a component but in fact they are more like a loop controller, therefore there are other circuits that can be used with the same properties as the LF's. The main purpose of this circuit is to establish the loop's dynamics and to deliver a suitable control signal to the VCO. The fact that filtering of unwanted components occurs is simply an additional task.

3.1.4 PLL Dynamics

To determine the PLL dynamics it is fundamental to calculate the loop's Transfer Function [45]. This model enables the analysis of the PLL's response. However, as mentioned before, a PLL is composed by nonlinear elements and shows an overall nonlinear performance and transfer functions only exist for linear systems [68].

Nonetheless, it is possible to use linear analysis techniques to study the loop's operation in certain conditions. Linear models can be applicable when the phase error between both signals is small, a condition normally achieved in lock state [45]. Therefore, the loop will be considered in lock conditions in order to develop the linear mathematical model.

To describe the dynamic system it is easier to consider it in the frequency domain and for that one can use Laplace Transforms tools to study and obtain the loop's transfer function [69].

Usually in electrical circuits a transfer function relates the voltages or currents of the input and output signals. When analyzing a PLL it has more interest to study the input and output in the phase domain.

Since one is dealing with a feedback network it may be difficult to define an output signal. From the definition of lock state, the loop operates in order to minimize the phase difference between the input signal and the VCO's output. Therefore, it is natural to assume the latter as the loop's output.

The easiest analysis is to study every component on Figure 3.6 independently and from there combine their transfer functions to obtain the overall PLL transfer function.

As described before in Section 3.1.1, the PD output voltage, assuming lock state and a linear component, can be approximated by Equation (3.2)

$$v_{pd} \approx K_d(\theta_i - \theta_o) = K_d\theta_e \tag{3.18}$$

Hence, the mathematical model of th PD is simply a zero-order block with a gain K_d and its transfer function is given by [45]

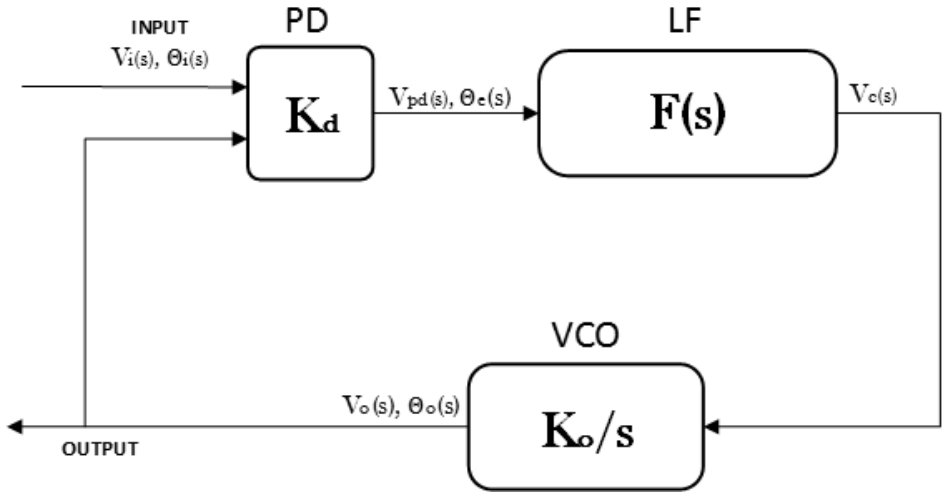

Figure 3.6: Mathematical model for the locked state PLL

$$\frac{V_{pd}(s)}{\Theta_e(s)} = K_d, \tag{3.19}$$

where $V_{pd}(s)$ and $\Theta_e(s)$ are the PD's output voltage (v_{pd}) and phase error (θ_e) projections in the phase domain.

On the other hand, the VCO behaves has a perfect integrator. From Equation (3.10) (and considering V_{co} null to simplify the analysis), the VCO's output phase θ_o will be the integral of the difference ($\Delta\omega_{io}$) between the input signal frequency and the VCO output (frequency is the derivative of phase), multiplied by the gain K_o, thus resulting in the transfer function [45]

$$\frac{\Theta_o(s)}{V_c(s)} = \frac{K_o}{s} \tag{3.20}$$

For the active filter described in Figure 3.5(c) its transfer function $F(s)$ is well known [60]

$$F(s) = \frac{K_f}{1 + s\tau_1} \tag{3.21}$$

where

$$\begin{cases} K_f &= -\frac{R_4}{R_3} \\ \tau_1 &= \frac{2\pi}{\omega_f} = C_2 R_4 \end{cases} \tag{3.22}$$

The model in Figure 3.6 enables the analysis of the PLL operation thus computing the system's transfer function $H(s)$ [46].

From feedback systems theory is possible to first determine the loop's forward gain $G(s)$ [60]

$$G(s) = \frac{\Theta_e(s)}{V_i(s)} = \frac{K_d F(s) K_o}{s} = \frac{K_d K_f K_o}{s + s^2 \tau_1} \tag{3.23}$$

Hence, the closed loop transfer function is given by [45]

$$H(s) = \frac{\Theta_o(s)}{\Theta_i(s)} = \frac{G(s)}{1 + G(s)} = \frac{\frac{K_d K_f K_o}{\tau_1}}{s^2 + \frac{s}{\tau_1} + \frac{K_d K_f K_o}{\tau_1}} \tag{3.24}$$

From systems theory it is possible to deduce that this PLL operates as a second-order system and so its transfer function can be compared to a general second-order transfer function $T(s)$ [68],

$$T(s) = \frac{\omega_n^2}{s^2 + 2\zeta\omega_n s + \omega_n^2} \tag{3.25}$$

Thus the loop parameters, i.e. the undamped natural frequency ω_n and the damping factor ζ are:

$$\begin{cases} \zeta = \frac{1}{2\omega_n \tau_1} \\ \omega_n = \sqrt{\frac{K_d K_f K_o}{\tau_1}} \end{cases} \tag{3.26}$$

These parameters will be the basis of the PLL's design. Defining from the beginning a set of performance parameters it is possible to compute the system's ω_n and ζ a thus establishing the desired performance for the loop- [45]. The designer can use these performance parameters to obtain the proper values of the components parameters (the gains K_d, K_f and K_o and the filter pole τ_1).

Although, most of these parameters are intrinsic to the characteristics of the chosen components and while some can be handled to best fit the desired performances, others are unchangeable (see Section 3.1.1 - Sequential Phase Detectors). With the chosen elements, as it will be explored in the next chapter, only the filter and VCO gains (K_f and K_o) and filter pole are adaptable. The PD gain is bounded by Equation (3.9) and so it is harder to adapt to the systems performance. This does not present a challenge, because K_f can be easily adapted to compensate if the remaining gains fall short of the required by the intended performance. For now both, PD and VCO will be considered as intrinsic properties of the chosen circuit and that cannot be changed. So the overall performance will only depend on the LF parameters.

As the main objective is to track transient frequency changes over time [42], it will be considered important to study the transient performance of the PLL. Hence, the

values of settling time (t_s) and maximum overshoot time (t_{max}) are considered with the same importance for performance specification. The settling time is the time elapsed from the application of a sudden input change until the output oscillation maintain within a previously specified error range. The maximum overshoot time is the period between the sudden input change and the highest value of the oscillatory response of the system.

Considering as satisfactory when the system oscillations decrease and remain in the interval of $\pm 2\%$ of the final value, t_s is given by:

$$t_s \approx \frac{4}{\zeta \omega_n} \tag{3.27}$$

The maximum overshoot is determined by finding the first zero of the derivative of the system output, and is described by

$$t_{max} = \frac{\pi}{\omega_n \sqrt{1-\zeta^2}} \tag{3.28}$$

Combining equations (3.26), (3.27) and (3.28) it is possible to define the values of the parameters of the PLL transfer function, and consequently the loop filter parameters:

$$\begin{cases} \zeta = \frac{{}^{4}/_{t_s}}{\sqrt{({}^{\pi}/_{t_{max}})^2 + ({}^{4}/_{t_s})^2}} \\ \omega_n = \frac{4}{\zeta t_s} \\ \tau_1 = \frac{1}{2\zeta\omega_n} \\ K_f = \frac{\omega_n^2 \tau_1}{K_d K_o} \end{cases} \tag{3.29}$$

The previous analysis assumes that the PLL operates as a linear system. In practice, the locking process may experience a nonlinear behavior during the initial part of its response. This nonlinear response may be significant and can dominate the locking operation.

This nonlinear behavior may be observed by the presence of cycle-slips. Cycle slipping occurs when the phase error grows faster than the loop can correct it, and can be observed in Figure 3.7.

This phenomenon is common for large frequency jumps and/or when the loop bandwidth is smaller compared to the loop's input frequency. For stationary input signals this effect is not significant, the only set back is a delay of the PLL's response, meaning higher locking times. Nonetheless, if the input is a fast non-stationary signal and this phenomenon is long enough than cycle-slipping can overcome the PLL

ability to lock into the signal frequency disabling its operation. Therefore, it must be monitored and, if necessary, measures to reduce it must be taken.

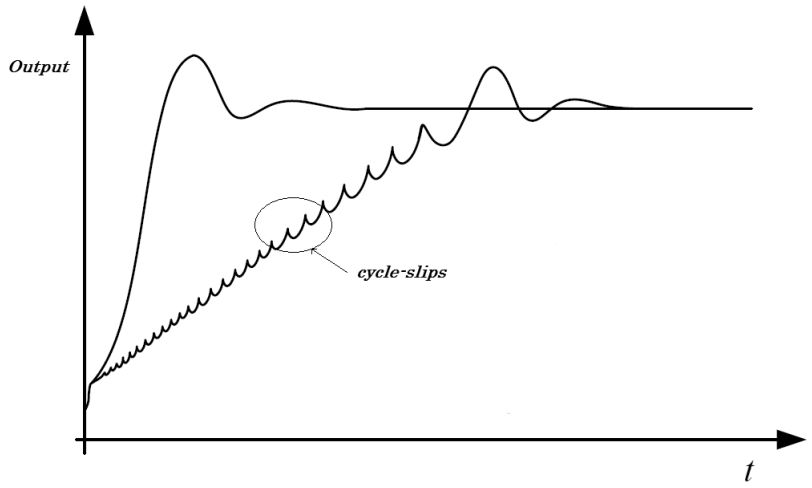

Figure 3.7: Operation of a PLL with and without cycle-slipping [63]. The fast growing curve corresponds to a normal PLL operation, while the other (with more oscillating events) corresponds to an operation under cycle-slipping phenomenon.

3.1.5 Definition of Performance Parameters

The definition of t_s and t_{max} defines the LF gain and pole which will be responsible for the restriction of the loops' performance [42]. The PLL's dynamic performance is governed by a set of key parameters related to the loop's bandwidth and response times. The PLL's Hold and Pull-out Ranges and Lock-in time are some of the parameters used to evaluate the performance [46].

Hold Range describes the PLL bandwidth, it is the range of frequencies in which the loop, once in lock state, can keep locked [46]. For EEG frequency tracking, defining an hold range identical to the input signal bandwidth will prevent the circuit to lock into spurious high frequency components that may not be efficiently removed by the preprocessing stage.

The Pull-out range is the minimum frequency step value applied at the reference input of the PLL to which a locked loop desynchronizes. For input signals that tend to change abruptly and for FM demodulation applications this parameter is important since it affects the circuit's ability to track components. For the EEG frequency tracking system the pull-out range should be high enough in order to be able to track events like unconsciousness or emergence where the EEG components tend in a smooth way to lower and higher frequency bands , respectively. But should be small enough to avoid tracking into high frequency spurious signals that usually result from noise sources.

The Lock-in time (T_L) is related to the time the PLL need to get locked and can be reasonably described by [46]:

$$T_L \approx \frac{2\pi}{\omega_n} \tag{3.30}$$

Nonetheless, the effective time that the PLL will take to lock into an input frequency will depend on the frequency itself. For higher frequencies, the circuit will have a better performance usually resulting in lower Lock-in times.

For the intended application is a less important parameter since during an anesthetic procedure common events are not abrupt but usually present a smooth evolution, although the system must have sensibility to eventual changes of state and detect them not too long after the occurrence.

In a previous Simulink® simulation of the PLL circuit [42] based on the model from Figure 3.6 it was found that an increase in t_s results in an increase of the hold and pull-out ranges. On the other hand, increasing t_{max} results in a deterioration of the PLL synchronization properties. Nonetheless, this increase leads to a decrease of the steady-state ripple.

From the conditions imposed to the PLL performance parameters, an operating point was found to satisfy those conditions, thus leading to the following values:

$$\begin{cases} t_s = 3s \\ t_{max} = 0.17s \\ \omega_n = 18.5 \\ \zeta = 0.07 \\ K_d = 1 \\ \frac{K_f}{\tau_1} = 2.66 \\ K_o = 128.7 \end{cases} \tag{3.31}$$

Which result in a Hold range of ±55 Hz relative to the reference (100Hz), a Pull-out range of ± 9.5 Hz and a Lock-in time of $0.34s$.

Since the cited paper was the starting point of the present work these parameters will be used as reference for the design of the PLL circuit for EEG frequency tracking in order to obtain a similar performance.

3.2 EEG Signals and Preprocessing

The EEG signal cannot be directly fed into the PLL circuitry due to several reasons. First, because, for anesthesia, useful components are within the range 0.5-47Hz and isolate the useful components of the signal [18]. Then because it is a very low frequency signal and, as it was referred above, PLL circuits perform best at high frequencies [47]. Last but not least EEG signals exhibit a variable amplitude over time and as it was shown in Section 3.1.1 that some components of the loop are sensible to this change in amplitude.

The loop requires a support circuit that prepares the input signal so it can be used in PLL applications. This section aims to present the types of solutions that can be used to solve these problems and those that were chosen to assemble this subcircuit.

Removal of undesired components can be achieved by the implementation of a LPF and a High-Pass Filter (HPF). Thus a baseband signal is attained. To transform the signal from baseband signal into a bandpass signal, an Amplitude Modulator is used resulting in a higher frequency modulated signal [70]. And since the PLL will operate as a FM demodulator amplitude components have no interest so the signal can be normalized to guarantee an uniform amplitude throughout the operation.

3.2.1 Filtering Stage

There are several filter topologies that can be implemented as the circuits for LPF and HPF [60]. Compared with a Chebyshev or an elliptic filter, the Butterworth filter has a slower roll-off, and thus will require a higher order to implement a particular stopband specification, but Butterworth filters represent a better compromise between attenuation and phase response [60,71]. These filters have a more linear phase response in the passband than other topologies can achieve.

For the required application, both filters (LPF and HPF) will be a 4^{th}-order Butterworth filters with a Sallen-Key configuration. Both designs are represented in Appendix B.

A Sallen-Key topology was chosen because it allows a simple design of second-order active filters. This configuration shows a smaller dependence of filter performance on the opamp's properties. Another practical advantage is that the ratio of the largest resistor value to the smallest resistor and the ratio of the largest capacitor value to the smallest capacitor are small [71].

A 2nd-order notch filter was also implemented to remove the 50Hz component introduced by the electrical grid. A Butterworth topology with a Sallen-Key

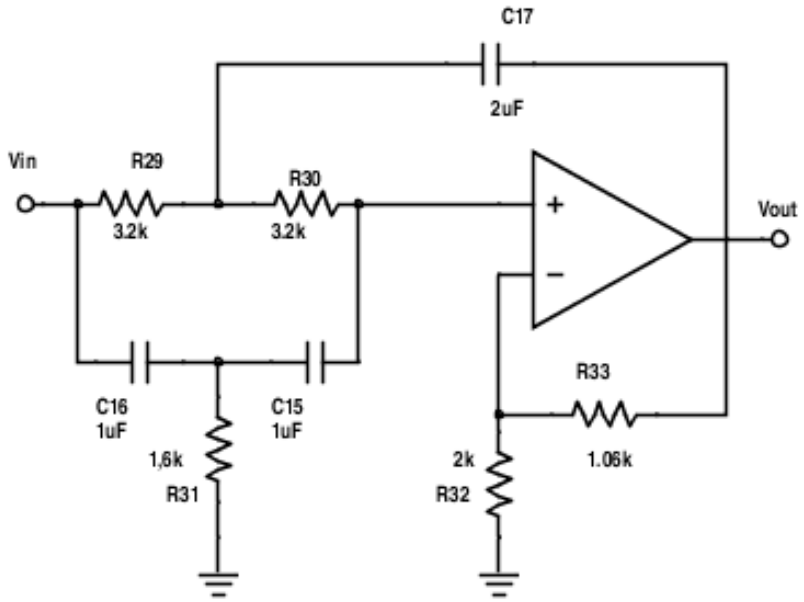

Figure 3.8: 50Hz notch filter

configuration was used to design the notch filter (Figure 3.8).

All the preprocessing stage filters were designed with the help of Texas Instruments FilterPro Design software.

3.2.2 Signal Modulation and Normalization

The modulation method to convert the input signal into higher frequencies must be by amplitude modulation because of the frequency demodulation properties of the PLL [44]. If the input EEG would be a frequency modulated (FM) signal then the circuit would only output the original EEG which would make no sense and it would not be useful.

There are two main ways to implement this type of modulation either by Double Sideband Amplitude Modulator (AM-DSB) or Single Sideband Amplitude Modulator (AM-SSB) [72]. The theoretical principles are similar between both methods, however the AM-SSB aims to remove one of the frequency bands (either the upper (USB) or the lower sideband (LSB)) of the modulated signal spectrum, as seen on Figure 3.9.

The AM-SSB has greater advantages because it allows bandwidth saving and lowers the signal total power. From a PLL point-of-view it has another advantage, since it narrows the bandwidth of signal to which the PLL is allowed to lock. This methodology prevents the PLL to lock into the carrier wave component and to an undesired frequency band of the signal, improving its performance. However it involves a more complex circuit, requiring more active and power consuming components [44].

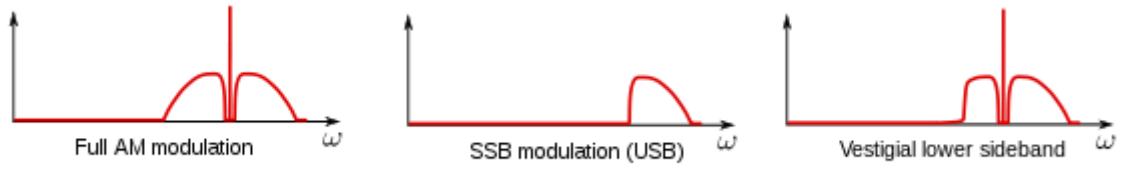

Figure 3.9: Frequency spectrum of the several modulation methods, on the left the DSB-AM spectrum, at the center the SSB-AM and on the right the VSB-AM. [70]

A AM-DSB, on the other hand, requires a quite simple circuit. A simple analog multiplier (e.g. the diode ring mixer on Figure 3.2(b)) can be used to implement this modulation. Comparing this example with the block design of a AM-SSB (Figure 3.10)it is possible to understand the difference of complexity between both methods [73].

A possible solution to replace the AM-SSB is through the implementation of a Vestigial Sideband (VSB) which is based on a AM-DSB circuitry but uses filters to remove one of the frequency bands and the carrier's frequency. It has a more simple architecture than a AM-SSB system, although the frequency band removal is not as efficient. A small portion of the band is still present (see Figure 3.9), thus the origin of the name "vestigial side band". Still the VSB is more stable when working with low frequencies unlike the AM-SSB [44].

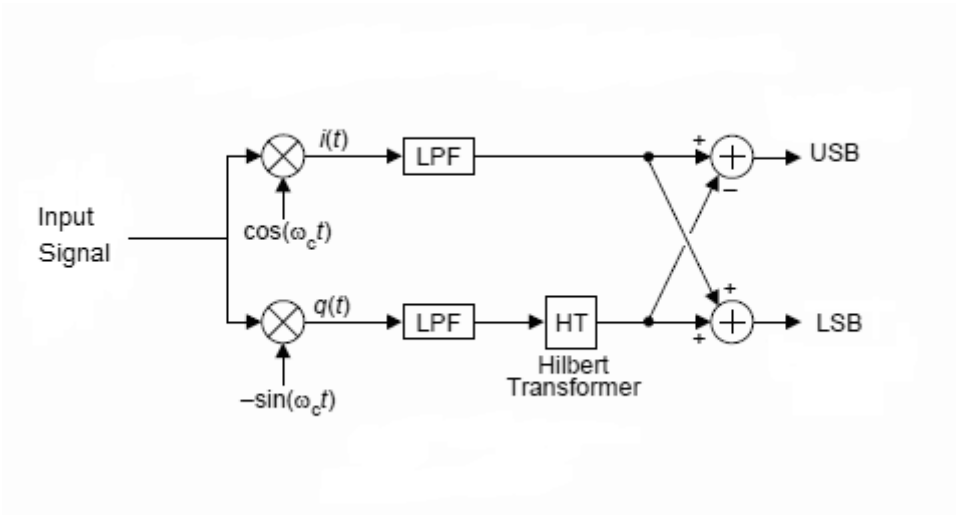

Figure 3.10: SSB-AM block schematic. The Hilbert Transformer block basically introduces a -90 degree phase shift to the signal. This is where the biggest complexity of the SSB monitor lies. ω_c is the carrier's frequency. [44]

Due to the complexity of the AM-SSB system a VSB circuit will be implemented as a solution to modulate the signal. The designed circuit is presented in Figure 3.11. The circuit uses an analog modulator based on the diode ring mixer from Figure 3.2(b)

to output a AM-DSB signal from the EEG input. Using a carrier wave at 100Hz the output results in a modulated signal centered at the carrier's frequency and with a bandwidth double the original input signal (approximately 53 - 147 Hz). However, as explained in Section 3.1.1 the mixer introduces several undesired frequency components so the modulated signal should bandpass filtered to isolate only the upper and lower sidebands. But since the aim is to obtain a VSB signal to save on the circuit complexity instead of using a band-pass filter to isolate both upper and lower bands and then use a HPF to remove the lower band and isolate the useful upper side band, it is possible to implement directly a band-pass filter centered at 124Hz with a bandwidth within 101 - 147 Hz approximately. A 6^{th}-order Butterworth filter with a Sallen-Key topology was the chosen solution for the band-pass filter (Appendix C).

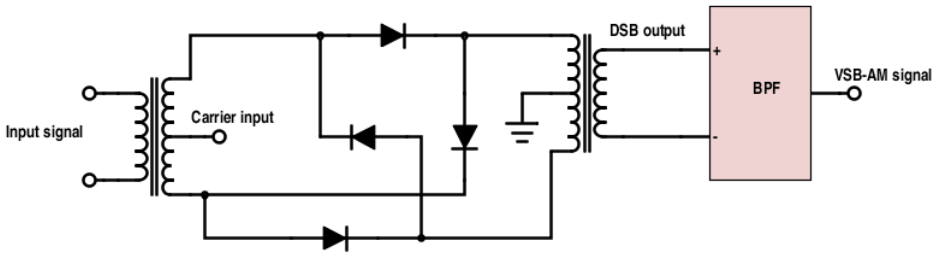

Figure 3.11: Schematics of the implemented VSB system

Once the signal is modulated it needs to be normalized mainly because of the PD operation. The use of a sequential PD simplifies the process. Since for this type of detector the amplitude of the input signals have no effect on the output and the only requirement is for them to be within 0V (volts) and the supply voltage (V_{cc}) then a possible solution should be through saturation (between 0 - V_{cc} volts) of the modulated EEG signal with a voltage amplifier.

3.3 Final Architecture

3.3.1 The Simulink model

Based on the mathematical model presented in Figure 3.6 and the performance parameters of Section 3.1.5, a Simulink® design of the proposed PLL was modeled.

Like it was explained in Section 3.2, this model also required a subset of components to prepare the input data to comply with the PLL's performance requirements. Hence, this model integrated the preprocessing LPF and HPF filters of Section 3.2.1 and a AM-SSB and normalization stages from Section 3.2.2, in addition to the PLL itself. Furthermore, it also had an artifact detector to remove external electrical interferences.

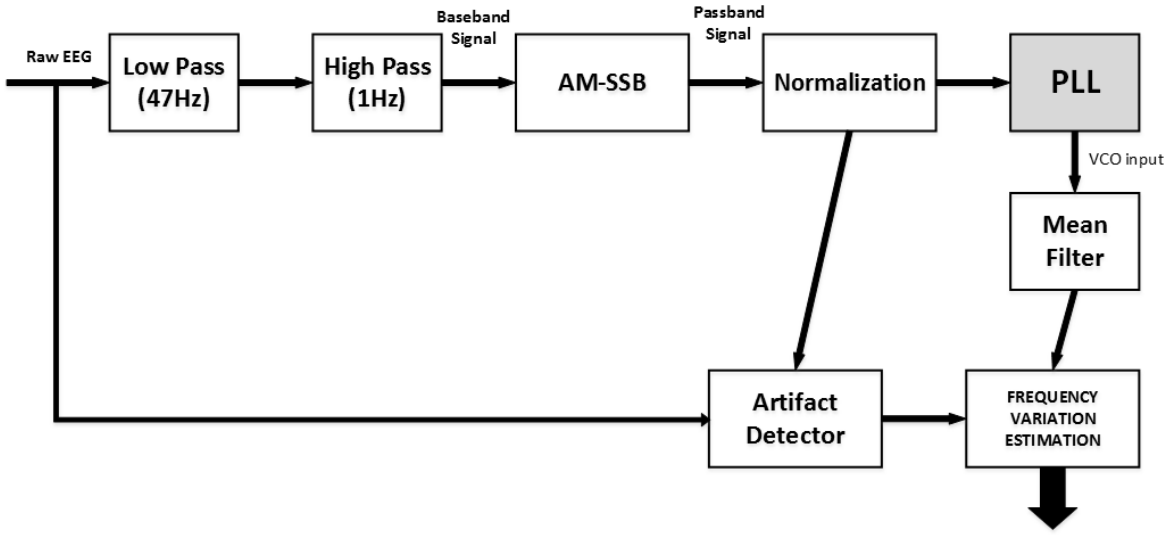

Figure 3.12: Implemented Simulink Model, adapted from [42]

This model can be observed in Figure 3.12, and it was first introduced in a previous work already cited in Section 3.1.5 [42].

The LPF and HPF components had the same specificities as those determined in Section 3.2.1, in other words, 4th order Butterworth filters were used as preprocessing filters. The modulator stage used a AM-SSB instead of the VSB modulator proposed in section 3.2.2. The artifacte detector employed a dynamic normalization, removing amplitude interferences and discarding highly contaminated EEG epochs.

3.3.2 The final analog design

Once the basic components are chosen then it is a question of assembling them together to design the final circuit.

First, to design the PLL the designer can start from the block diagram presented in Figure 3.1. The chosen component for the PD was the Phase-Frequency Detector. Though it is more complex it has a better tolerance to noise in the signal. The 555-astable oscillator will be used as the loop's VCO since it has the best performance at low frequencies and short bandwidths and an active first order filter will be the LF to help the designer adjusting the loop gain.

Then its just a matter of adapting these components to the specifications of the application.

In Equation (3.15) is described the dependence of the astable's period of oscillation with the control voltage v_c and three passive components (R_1,R_2 and C_1). The control voltage can vary between 0 and V_{cc}, so by defining a center frequency for the oscillator and its bandwidth it is possible to determine the astable passive elements

$$\begin{cases} R_1 = 100k\Omega \\ R_2 = 25.5k\Omega \\ C_1 = 235nF \end{cases} \tag{3.32}$$

The LF components (R_3,R_4 and C_2) can simply calculated from (3.22) and (3.29) using as reference the previously defined parameters in (3.31).

It is important to mention once again that the effective practical gains K_d and K_o may not correspond to the expected values in Equation (3.31) since they are an intrinsic property of the components. To compensate these differences the LF gain K_f can be adapted. However, changes in K_f will have repercussions in the values of the filter passive elements where certain gain values will translate in less practical values for these components. The designer must have in mind that a compromise between the gain and the component values must be achieved in order to have the desired performance but at the same time facilitate the practical assembly of the circuit.

Basing the filter design on this principles the compromise achieved for the application resulted in the following values for the filter components

$$\begin{cases} R_3 = 100k\Omega \\ R_4 = 25k\Omega \\ C_2 = 10\mu F \end{cases} \tag{3.33}$$

Since all the basic components of the final PLL circuit are defined it is possible to assemble them following the block structure of Figure 3.1. Then it is just a question of assembling the preprocessing circuits mentioned in Section 3.2.2 to prepare the input signal to the specifications of the PLL. The final architecture is presented on Figures 3.13 and 3.14.

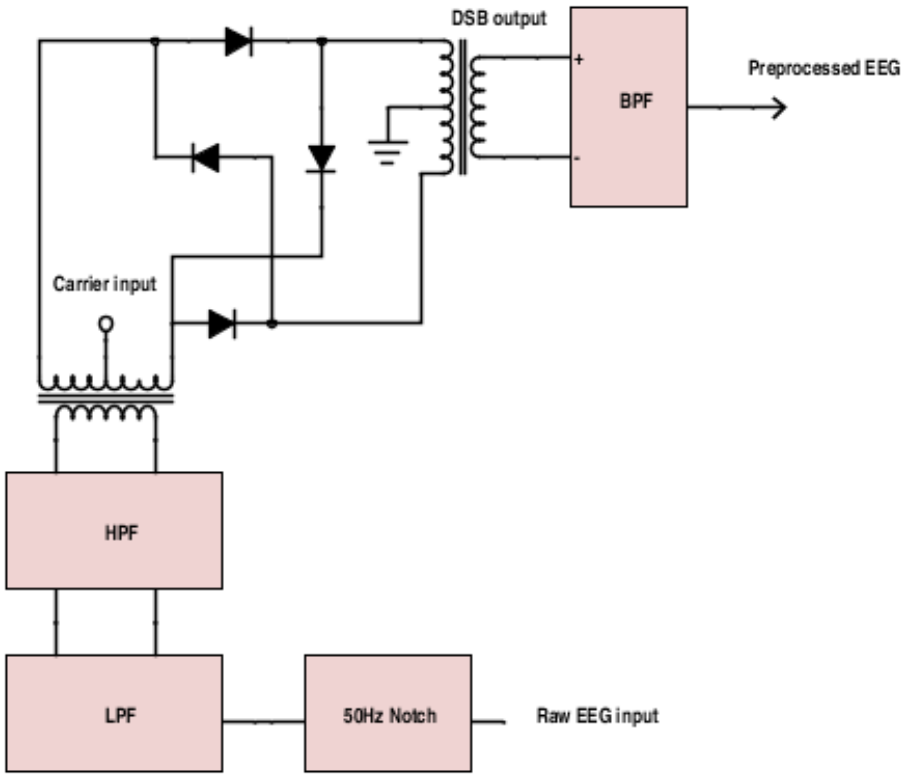

Figure 3.13: Final Architecture's preprocessing stage

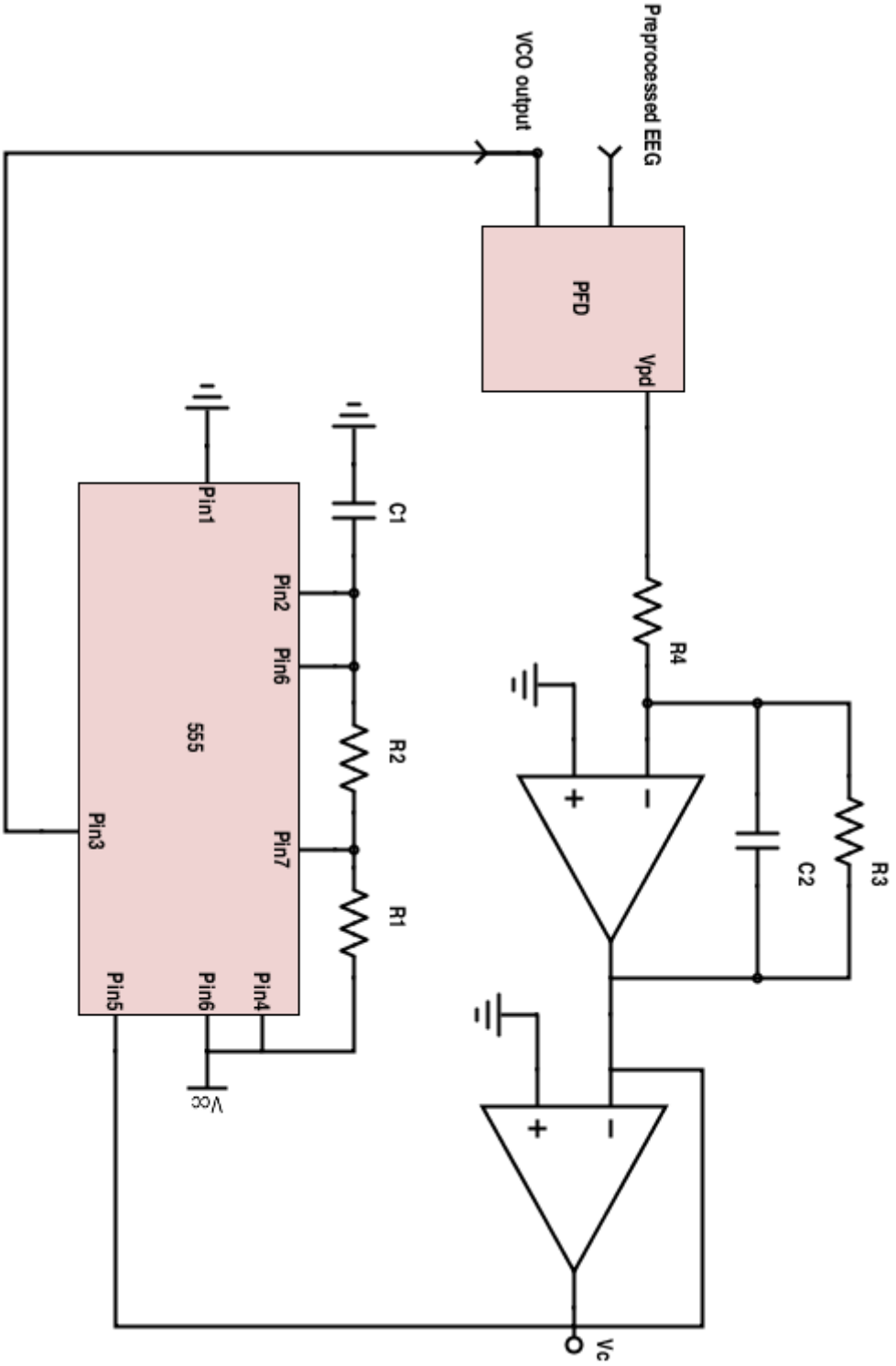

Figure 3.14: PLL's Final Architecture

Chapter 4

Results and Discussion

Once the PLL dynamic model is computed it is possible to implement and test it. A software model had already been implemented [42], and validated the model. Nonetheless, some tests were performed with this model, using real EEG signals collected from patients under general anesthesia. This model was used to test the performance of the preprocessing subcircuit components and the designed PLL circuit.

The next step required the implementation of the final circuit, first in a SPICE-based software for simulations and then in the analog assembly.

The EEG signals were collected using electrodes over the scalp according to the 10-20 system, with standard instrumentation, that sampled it at a 256Hz rate [9].

4.1 Simulink Model

The assembly of high order filters is quite impractical in an analog circuit. Therefore, and since EEG signals tend to be highly noisy, one must find a compromise between a good noise removal and the order of the filter.

Digital signal processing tools have the advantage in this process since they can simulate analog filters performance, easing the process of filter choice and evaluation.

In Section 3.2.1, 4th-order Butterworth filters were chosen to preprocess the EEG signal before it is fed into the circuit. In addition to this, a 6th-order bandpass Butterworth was presented as the Modulation system filter to remove the carrier and the lower band components. The software model, based on Simulink® and MATLAB® tools (MathWorks Inc., USA), was mainly used to evaluate if the chosen filters were adequate.

The digitized EEG signals were first filtered with the notch filter from Figure 3.8 to remove the 50Hz component. Then it was bandbased first using the 4th-order

Butterwoth filters. Lower order (2nd and 3rd) filters were also tested to assess if they could be used in an analog circuit. Afterwards, the baseband signal is modulated into a bandpass signal with a VSB process. The VSB system requires a bandpass filter to isolate the desired upper signal band.

Both raw and filtered EEG signals were compared through spectrograms, which represents the frequency spectrum of a signal over time.

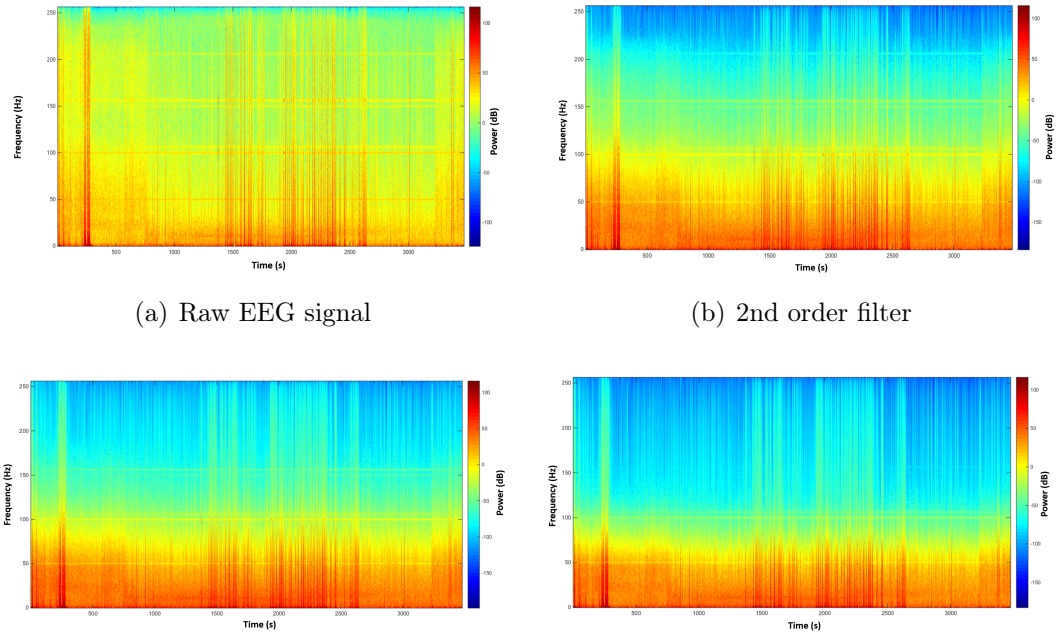

(a) Raw EEG signal

(b) 2nd order filter

(c) 3rd order filter

(d) 4th order filter

Figure 4.1: Spectrograms of a raw EEG signal with low noise and after preprocessing with several different order filters. All filters have a Butterworth topology. The colored bar, at the right, describes the power (dB) per frequency component.

Since the signals were collected at a sample rate of 256Hz, they will contain frequency components within the range of 0-128Hz. However, we are only interested in a useful signal approximately within 1-47Hz, for the baseband signal, and within 101-147Hz, for the bandpass signal. Therefore, filters with steeper roll-offs are better at delimiting shorter bandwidths. However, the steeper the roll-off the higher the filter order will be.

Through a spectrogram it is possible to evaluate the performance of each filter on isolating the desired bandwidth.

The spectrograms shown in Figure 4.1 represent a signal with low noise content. For this kind of signal, a 2nd-order Butterworth presents an acceptable performance, though it does not totally remove some components higher than 50Hz. The 3rd and 4th order filters have better performances, as it was expected, specially the latter.

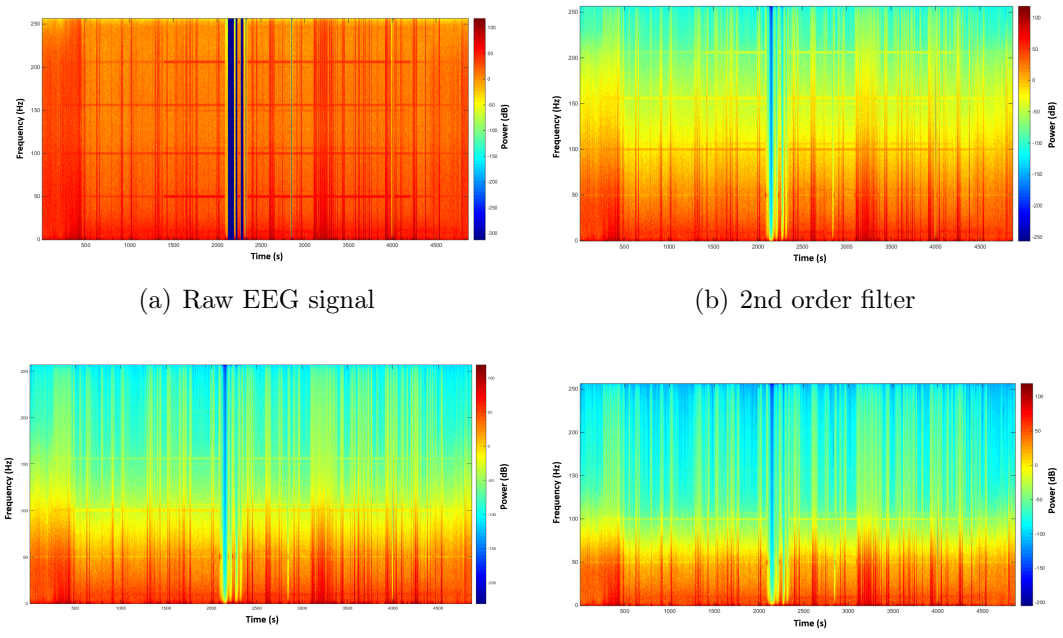

(a) Raw EEG signal

(b) 2nd order filter

(c) 3rd order filter

(d) 4th order filter

Figure 4.2: Spectrograms of a raw EEG signal with high noise and after preprocessing with several different order filters. All filters have a Butterworth topology. The colored bar, at the right, describes the power (dB) per frequency component.

For high noise signals identical to the signal represented in the spectrograms in Figure 4.2, a 2nd-order filter has a poor performance, whilst a 4th-order shows the best one, though not removing completely higher components.

Therefore, for a general purpose circuit a 4th-order Butterworth signal is the best option since it has a good performance isolating the desired signal bandwidth, without imposing to much burden to the circuit.

The 6th-order bandpass is analyzed in Figure 4.3. The spectrograms of the signal throughout the modulation process are shown. Comparing Figures 4.3(a) 4.3(b) one is able to identify the frequency shift between the baseband and the bandpass signal after amplitude modulation. As expected, from Figure 4.3(c) it is possible to observe that the bandpass filter of the VSB system do not remove completely both carrier and lower band components, as expected.

Next, the Simulink model was tested using four EEG signals collected from patients under general anesthesia.

When the input is a mixed signal, PLL circuits have the ability to track different components depending in the VCO's initial frequency. Therefore, the circuit will have different performances depending on the initial conditions of operation. For different initial frequencies the PLL exhibits different profiles, as seen on Figure 4.4 i). Thus, it

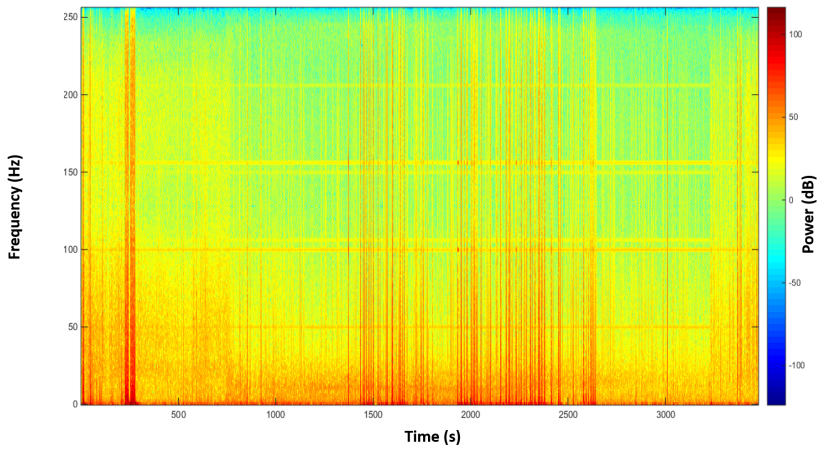

(a) Raw EEG signal (baseband signal)

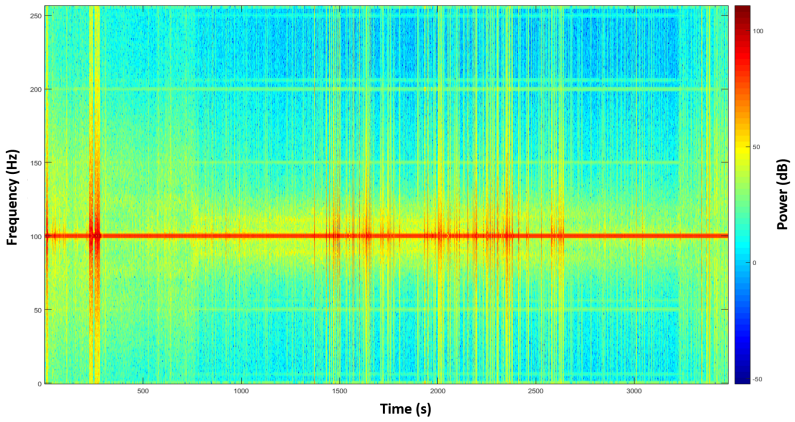

(b) EEG signal after AM-DSB (bandpass signal)

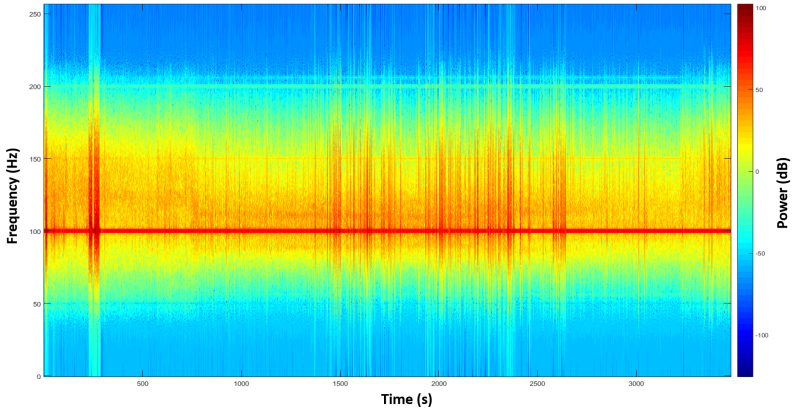

(c) Resulted VSB signal after filtering

Figure 4.3: Spectrograms of a raw EEG signal before (a) and after (b) amplitude modulation and after carrier and lower band components removal, with the 6th order bandpass Butterworth. The colored bar, at the right, describes the power (dB) per frequency component.

is possible to combine these different profiles to observe a time-frequency map similar to a spectrogram.

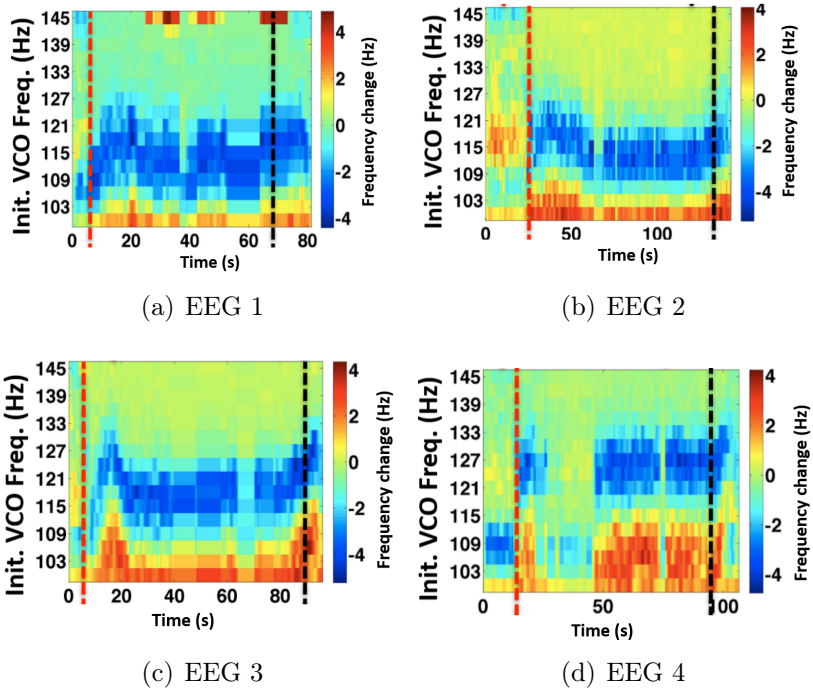

(a) EEG 1 (b) EEG 2

(c) EEG 3 (d) EEG 4

Figure 4.4: Results obtained for four patients. Shows the PLL profiles for several initial VCO frequencies, obtained with the Simulink model. The colored bar represents the frequency change (Hz) obtained by multiplying the input VCO voltage with the gain K_o (in Hz/V). The vertical dashed red line indicate the approximate starting of anesthesia and the black line the beginning of the recovery period.

4.2 Circuit Design and Software Simulation

Before assembling the complete circuit, every component was simulated using the SPICE-based TINA® software owned by Designsoft and Texas Instruments.

Each component has its own parameters to be evaluated. For the PD only the gain K_d needs to be studied. The VCO however requires attention to the linearity of its operation, through the analysis of a characteristic curve, and to the K_o gain.

4.2.1 Phase Detector (PD)

The PD gain can be calculated from (3.9). Using a supply voltage V_{cc} of 3.3V the PD gain is then obtained

$$K_d = \frac{3.3}{4\pi} \approx 0.26(V/rad) \tag{4.1}$$

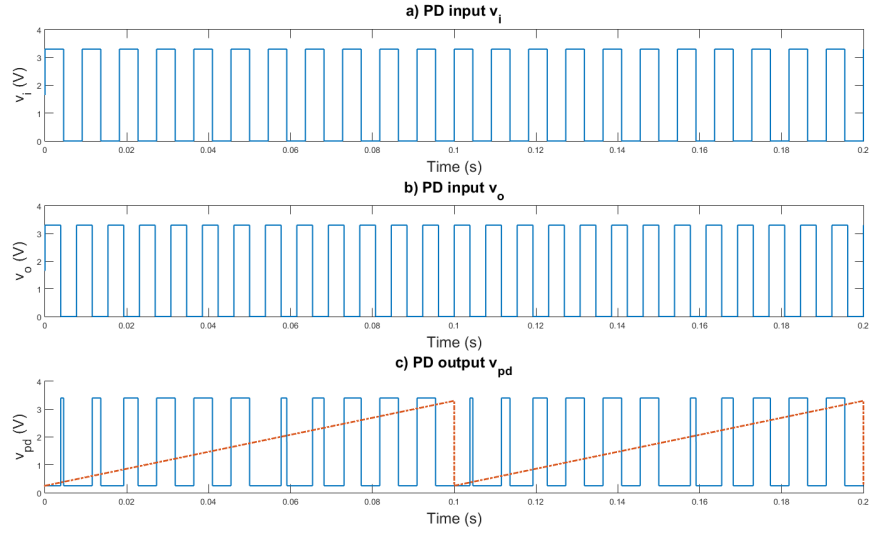

Figure 4.5: A typical output of the chosen PD. The inputs v_i (a)) and v_o (b)) have a difference of 20Hz between them. In c), is possible to observe the output v_{pd} represented by the square wave, and a red dashed line that shows the output voltage component that is proportional to the phase error θ_e.

It is a lower gain than the expected in Section 3.1.5. However the difference can be compensated with the LF gain.

A typical output for the chosen PD is presented in Figure 4.5. It is possible to observe that the output v_{pd}, in this case a square wave, is composed by several components. One of these components is the voltage directly proportional to the phase error between both inputs.

4.2.2 Voltage Controlled Oscillator (VCO)

To test the VCO performance, simulations were made by injecting a constant DC voltage into the VCO control pin and determining the output frequency wave. For an ideal component the control voltage would be able to vary between 0 and V_{cc} volts. However for the designed astable due to the voltage drop of approximately 0.7V of the internal transistor than the input control voltage can only vary between 0.7 and (V_{cc}) volts. Through this test it is possible to evaluate the VCO bandwidth and gain (K_o). The simulated results are shown in Figure 4.6.

At a first look was found that the designed oscillator could generate signals with frequencies between 13.7 - 164.5 Hz. Our application only requires a bandwidth of approximately 100-150Hz.

Secondly, Figure 4.6 shows that the output frequency is not linearly proportional

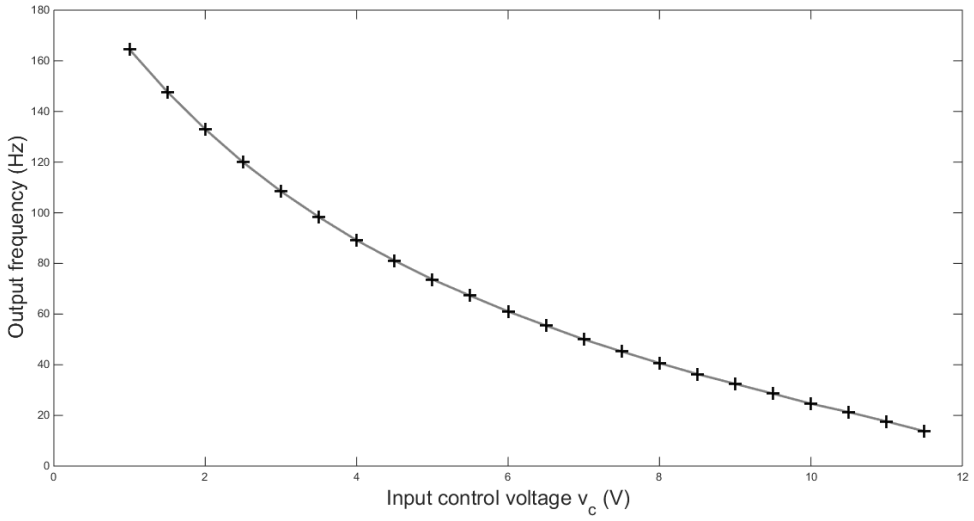

Figure 4.6: VCO characteristic curve.

to the input voltage just like it was previously predicted by equations (3.14) and (3.15). Although it allows the determination of the VCO bandwidth, this relation complicates the calculation of the gain K_o. To overcome this problem, and since the real bandwidth (13 to 164 Hz) is bigger than the necessary for our application (between 100 and 150 Hz), it is possible to select a smaller range of the VCO characteristic that includes the desired bandwidth and where its linearity can be assessed. This delimitation, denominated as Range of Interest (ROI), considers a control voltage v_c variation between 1.5 and 3.5V, which corresponds to a bandwidth of 98 to 148Hz. Thus, the characteristic on Figure 4.7 is obtained.

In the ROI, the VCO behavior is more identical to the desired performance. Although the output frequency variation is not completely linear against the input voltage, by a linear fitting it is possible to achieve a curve with a R-square value of 0.9945. The R-square value gives information about the goodness of fit of the curve to the data and the attained result is good enough to accept the determined ROI as a linear region. The fitting algorithm returns the following first order equation

$$f_{vco}(v_c) = -24.66v_c + 183.1 \tag{4.2}$$

If the other components (PD and LF) are well designed then the oscillator will never operate outside the ROI. Therefore it is possible to consider this ROI as the effective VCO characteristic, delimiting the bandwidth to 98.3 - 147.7 Hz. And since this new characteristic is linear it is possible to determine an approximation to the gain K_o adapting Equation (3.10). If Δv_c is the variation of input voltage and Δf_o is the delimited VCO bandwidth then the gain can be computed by:

$$K_o = 2\pi \frac{\Delta f_o}{\Delta v_c} = -155.1(rads/V) \tag{4.3}$$

As seen in Section 3.1.5 the expected value for the gain K_o was 128.7. Nonetheless, the extra gain in the designed VCO can be compensated decreasing the LF gain. Another detail is the negative gain value. This will not affect the overall performance of the circuit. From the circuit transfer function in equation (3.24) the only effect that the negative sign will have is a decreasing response. This means that for an increasing input frequency the PLL output voltage will decrease.

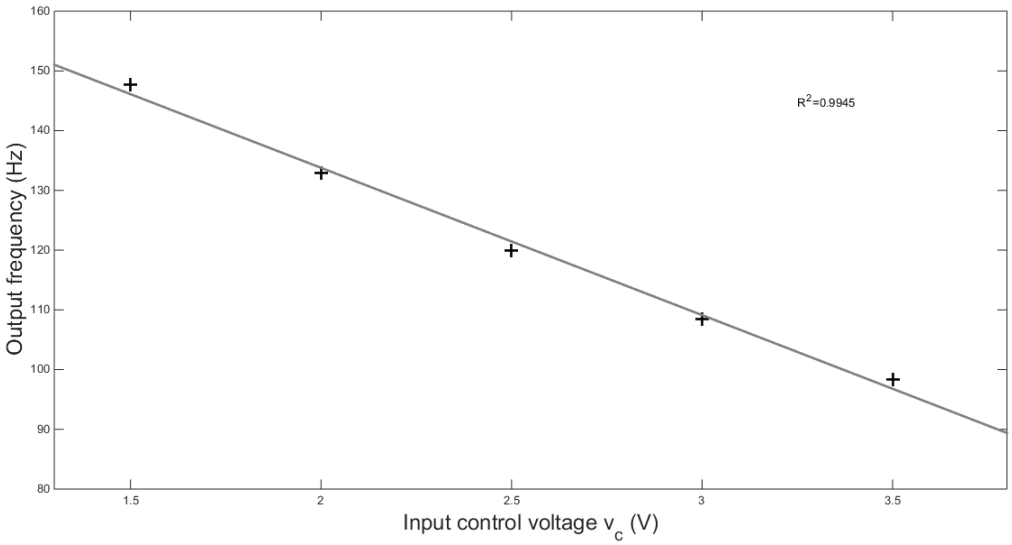

Figure 4.7: Range of Interest of the VCO characteristics

4.2.3 PLL Analysis

To determine the PLL operation and performance first it can be subjected to several tests either using single frequency or mixed (various frequency components) stationary signals or even non-stationary signals. From these tests, it is possible to calculate the loop's hold and pull-out range and lock-in time.

The hold range can be determine through a sweep test. This technique involves the injection of a frequency ramp at the PLL input. The frequency values to which the loop can retain lock will correspond to the PLL Hold range.

The pull-out range is computed by continuously input several different frequency steps. The minimum step value that results in a loss of lock state determines the pull-out range.

Lock in time can be predicted in (3.30) (Section 3.1.5) and it can be highly

influenced by the presence of cycle-slipping. Furthermore, it must be taken into account this parameter is defined considering that the loop is in lock conditions which assumes small phase errors. However if the input signal has a higher phase difference relatively to the VCO output than the lock-in process will take longer, demanding more operation cycles from the loop.

Performance Tests with Single Frequency Components

Injecting into the circuit a single frequency signal leads the loop to enter into an unlock state. The PLL operates in order to minimize the phase difference between the input and the VCO output. In a lock state, the phase difference is minimum (nearly zero) and it is possible to output a near DC voltage from the loop, at the VCO control pin. The voltage level of the PLL output (which is in fact the VCO input control voltage) will be specific to the input frequency. Changing the input frequency and allowing the loop to lock into it, makes it possible to determine the PLL characteristic, in other words, the output voltage (VCO input voltage) as a function of the input frequency. From the loop's characteristic, it is also possible to calculate the hold range.

To determine both performance elements it was performed a sweep test, by considering as input a single frequency non-stationary signal. This means that the input signal starts with a previously determined frequency f_1 which is then continuously increased or decreased to another frequency f_2, covering the entire range $f_1 - f_2$.

Due to limitations of the simulation software, instead of a continuous sweep a discrete series of 5Hz frequency steps using a square wave input was used. From data collected using TINA software simulator the PLL characteristic was computed considering only the circuit Hold range. The results are presented in Figure 4.8, and it was found that the simulated PLL can retain lock within the frequency range of 100-150Hz.

Using a linear fitting algorithm the PLL output voltage in response to the input frequency change (Δf_{in}), relative to the carrier frequency (100Hz) was analyzed in order to evaluate the linearity of the circuit. With a R-square value of 0.993 returned by the linear fit, then the PLL is assumed to have a good linear operation for the frequency range 100-150Hz. The following first order equation was calculated

$$v_{out}(f_{in}) = -0.03915\Delta f_{in} + 3.248 \tag{4.4}$$

In fact, this range was determined as the loop Hold range. Outside this range the loop would present abnormal operation and inability to lock into the input frequency.

It is also expected that the slope of the linear model in Equation (4.4) and the characteristic in Figure 4.8 should be equal or near to $2\pi/Ko$, which was confirmed.

As one can see from Equation (4.4) and Figure 4.8, the negative slope of the PLL response is a result of the VCO negative gain, as mentioned in Section 4.2.2.

Another detail that was taken into consideration and measured was the VCO frequency when the loop was locked. In theory, in lock conditions the VCO output frequency should be equal or very close to the input frequency (because of the minimization of phase error). From Table 4.1 and Figure 4.8 is possible to compare both frequencies and determine the error between them when the loop is considered in lock.

The differences on Table 4.1 between the input and VCO's frequencies are probably caused by the VCO's non-linear response. Nonetheless, these differences are never higher than 2%, a valuable which can be considered acceptable for the application.

Table 4.1: Frequency error between the input signal and the VCO output frequencies

Input Frequency (Hz)	VCO output frequency (Hz)	Frequency error (%)
100	99.30	0.70
105	104.20	0.76
110	109.80	0.18
115	114.50	0.43
120	120.05	0.04
125	123.00	1.6
130	129.40	0.46
135	136.60	1.19
140	139.47	0.38
145	145.99	0.68
150	152.43	1.62

Figure 4.9 shows an example of the PLL's simulated response. The output frequency variation is represented through time, with a constant input of 130Hz. It is possible to observe the presence of cycle slips during settling. As explained in Section 3.1.5 this phenomenon occurs because the phase error is higher than the capacity of the loop filter to correct it. This will cause a delay on locking operation, increasing the settling time. If present in the physical circuit, and if it turns to dominate relatively to locking time, this effect will have negative consequences in the overall performance of the circuit.

However, the fact that the simulation presents cycle slips does not guarantee that the physical circuit will have it too. It is believed that in the simulation the cycle slips occur because of the circuit's initial conditions, specially the VCO's. During

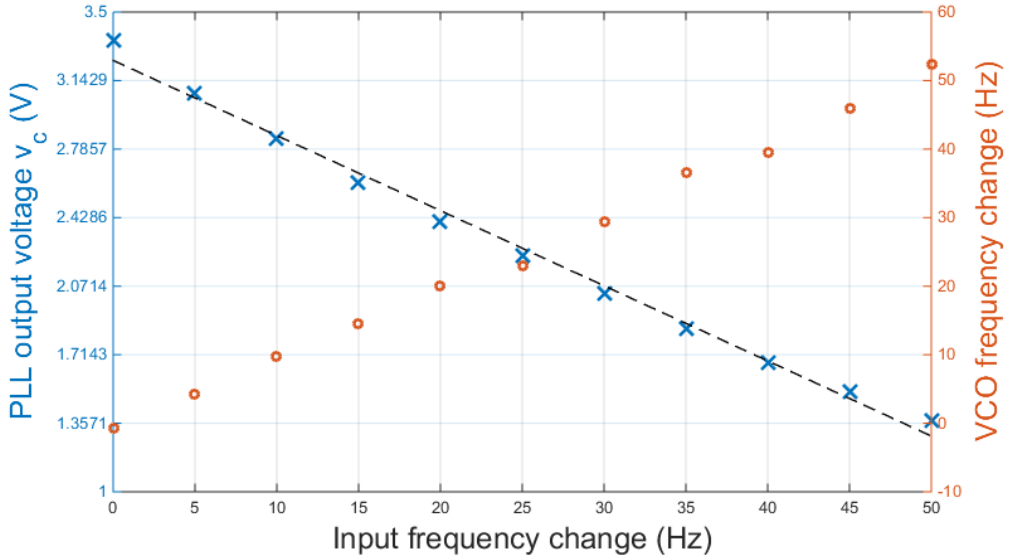

Figure 4.8: In blue (cross marks) is represented the PLL output voltage in function to a determined fixed input frequency. The dashed line represents the linear fitting representing the PLL characteristic. In red (round marks) is represented the VCO output frequency when the PLL is in lock state.

simulations the software used the default conditions which for the VCO resulted in a non-oscillatory state (frequency of oscillation was zero). However, real VCOs have shown to oscillate natural even if the input voltage is null. Thus the simulations, for the frequency range in test, will always generate cycle slips.

During simulations it was possible to observe that for lower input frequencies, settling time was higher. As it was mentioned above the VCO starts simulation with no oscillation so one would be led to assume that for lower frequencies (which result in lower phase errors) the settling time would be lower. Still there is a reason for the PLL to use modulated input signals. At lower frequencies the loop tend to have a slower response. The higher is the frequency the faster the PLL will lock into it even in the presence of cycle-slipping. Furthermore, it was also detected that for higher frequencies the cycle-slipping time (pull-in time) is lower. The loop shows a faster correction of the phase error which is in accordance with what was mentioned above.

Relatively to the pull-out range, this parameter could not be determined. The TINA software does not allow the change of the input frequency during simulation. Therefore, it was not possible to apply frequency steps, thus preventing the determination of the pull-out range.

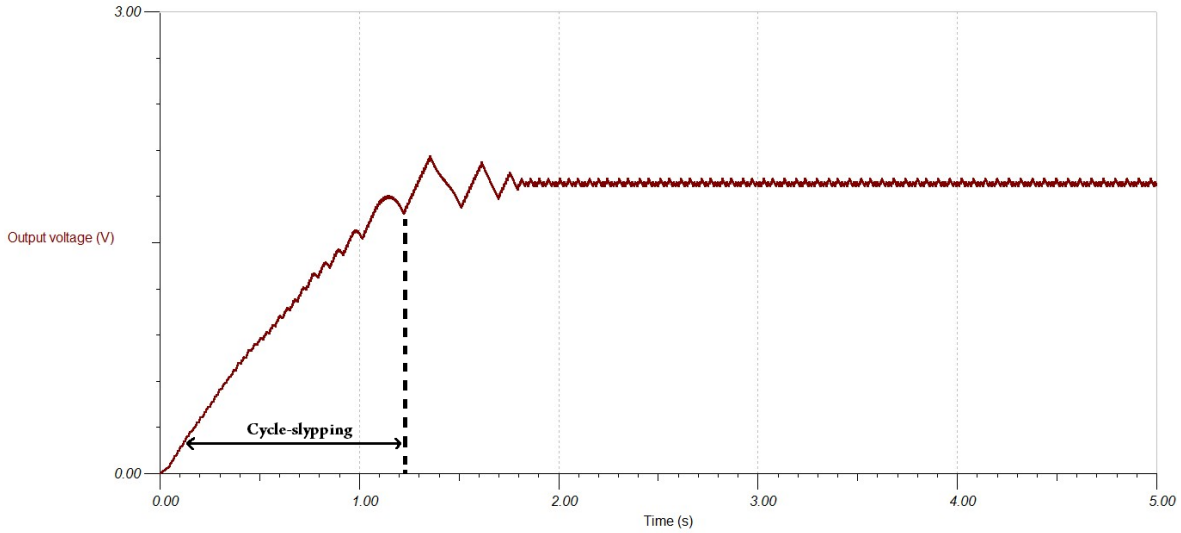

Figure 4.9: Evidence of cycle slips in the PLL simulated operation.

4.2.4 Conclusion

Using the TINA simulator was possible to design and test the planned circuit, in order to evaluate some performance parameters. First, the individual components were tested. The VCO requires special attention since it should present a near linear operation. This component was proven to have a good linear response within the intended frequency range. The obtained gain K_o of -155.1 $(rads/V)$ was near the values proposed by a previous implementation [42], as well as the computed PD gain K_d of 0.26 V/rad . The differences between the expected values and the real ones are compensated through the filter gain K_f. The negative VCO gain does not affect the overall performance. It only causes the PLL output voltage to decrease with an increase in the input frequency.

Once the individual components' properties are validated it is possible to join them as the intended PLL schematic and then test the overall performance (linearity, hold and pull-out ranges and lock-in time).

Through a sweep test the PLL was shown to have a good linearity and a hold range of ±50Hz, broad enough for the application. However, the pull-out range could not be calculated using the simulation software and the presence of cycle-slipping did not allow the determination of the lock-in time.

Do to this difficulties, the performance parameters will be better tested in the physical circuit.

4.3 The Physical Circuit

The analysis of the physical circuit is identical to those performed in the simulator. The performance parameters are the same (linearity, hold and pull-out ranges and lock-in time) as well as the tests performed. Hold range and linearity will be tested through a sweep test and pull-out range through a series of frequency steps until the loop loses lock.

The tests were performed using the Analog Discovery® (Digilent Inc., Pullman, WA, USA) device which can operate as both signal generator and acquisition board. MATLAB®'s Data Acquisition Toolbox (MathWorks Inc., USA) and WaveForms® software (Digilent Inc., Pullman, WA, USA) were used as support software for signal generation and data acquisition.

4.3.1 Voltage Controlled Oscillator (VCO)

The physical VCO was tested through the same method used in the simulation. Through the input of constant DC voltages and using the Waveforms software to exhibit real-time frequency spectrum of the VCO's output. The results are shown in Figure 4.10

Figure 4.10 shows that the VCO performance is identical to the one expected in Section 4.2.2. Although the output frequency variation is not completely linear against the input voltage, by a linear fitting it is possible to achieve a curve with a R-square value of 0.9916. The fitting algorithm returns the following first order equation

$$f_{vco}(v_c) = -29.45v_c + 195.1 \tag{4.5}$$

Then, it is possible to determine an approximation to the real gain K_o following the same logic in Section 4.2.2:

$$K_o = -188.81(rads/V) \tag{4.6}$$

4.3.2 Loop Dynamics

Hold Range and Linearity

Testing the circuit with a sweep test, as it was done in the simulator software, both PLL characteristic and hold range can be determined. The sweep test injected a square wave signal with frequency ranging from 100 to 200Hz. The results are shown in Figure

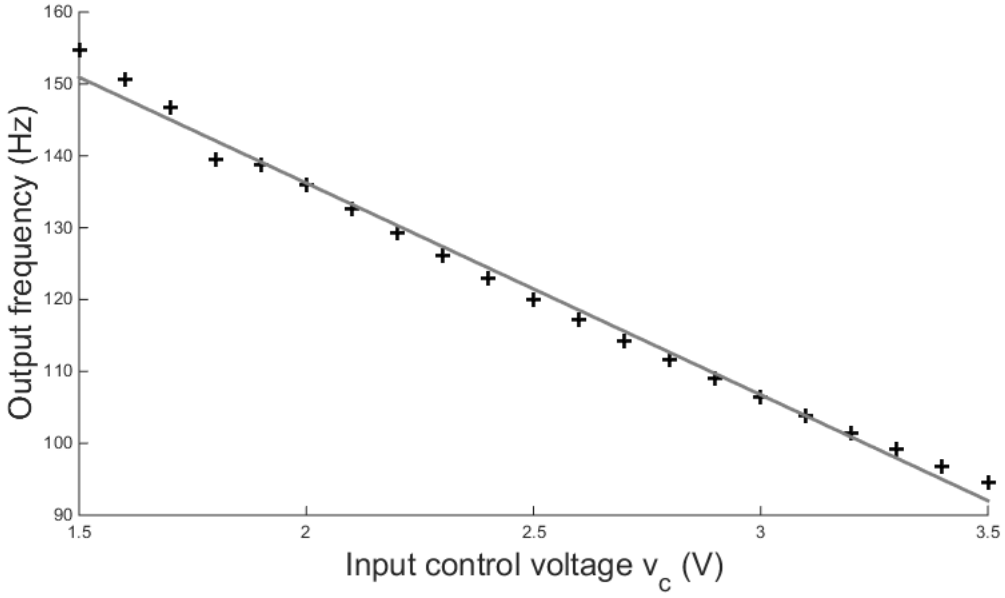

Figure 4.10: Characteristic curve of the analog VCO

4.11.

From Figure 4.11 it possible to observe the loop linear operation similar to the one simulated in Figure 4.8 though this linear region is contained within a limited range of frequency. This range can be denominated as the PLL's bandwidth or hold range. The physical circuit presents a hold range of ±55Hz (5Hz more than the simulation). Isolating the linear region from the out of lock regions (Figure 4.11(b)) it is possible to compare this characteristic response to the simulation. Outside this regime the loop is out of lock. False lock states can be observed at higher frequencies.

Through linear fitting of the recorded data resulted the following first order equation

$$v_c'(f_{in}) = -0.03362\Delta f_{in} + 3.013 \tag{4.7}$$

The fitting algorithm returns a R-square value for the line described by (4.7) of 0.993.

Once again the slope of the characteristic response input frequency change - output voltage in Figure 4.11(b) should be equal to $2\pi/K_o$.

Pull-out Range

It was tested and observed that the designed PLL in a lock state could not lock into signals if the frequency step was of ±20Hz relatively to the previous frequency.

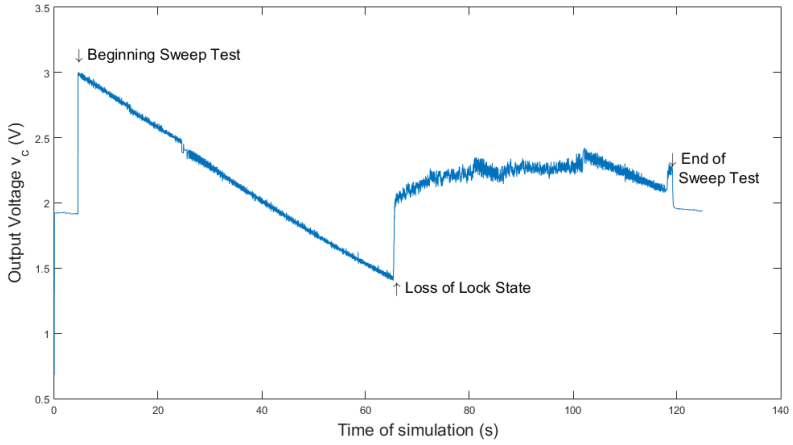

(a) Sweep Test

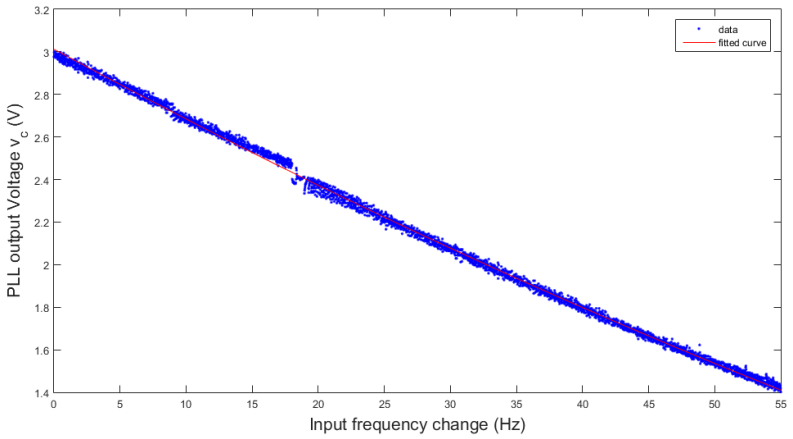

(b) Linear Range

Figure 4.11: In (a) is presented the PLL response to sweep test with an input frequency variation from 100 to 200Hz. The linear regime on (a) is shown with more detail in (b) and corresponds to the PLL lock state.

Lock in Time

No cycle-slipping is observed on the analog PLL circuit. Thus it is easier to determine the real lock-in time (T_L). The circuit's lock-in times were tested using several input frequencies and describe the period between the injection of the signal and the time in which the output voltage settles (PLL is locked). The results are presented in Table 4.2.

Table 4.2: Lock-in times of the circuit, for different input frequencies.

Input frequency (Hz)	Lock-in Time T_L (s)
100	1.49
105	0.82
110	0.71
115	0.66
120	0.74
125	0.43
130	0.72
135	0.72
140	0.43
145	0.36
150	0.18

From Equation (3.30), it was expected that the value of T_L would be approximately 0.34s. The determine values, listed in Table 4.2, are somehow discrepant from the expected value. As it was mentioned, the PLL's performance varies depending on the frequency of operation. The practical results in Table 4.2 support this claim.

4.3.3 Conclusion

The analog VCO has a higher gain than expected (-188,81 instead of 155,1 rads/s) though it does not affect the overall PLL operation, as one can see comparing Equations (4.4) and (4.7). Thus comparing both equations, one is led to conclude that the implemented physical circuit operates as expected by the simulations.

Nonetheless, it would be expected that the slope of the PLL characteristic should be equal to $2\pi/K_o$, which is observed. The slope of the characteristic returns a gain K_o of -186.88 (rad/s), corresponding to a relative difference of 1.02% to the gain calculated in Equation (4.6), which is acceptable.

Both linear response and hold range are according to the desired. A higher hold range may be a result of non ideal components in the circuit.

Regarding the Lock-in times, as it was expected, the lower is the input's frequency the higher is the lock-in time. For higher frequencies the circuit has a better performance at tracking frequencies. Furthermore, low lock-in times like those returned by the designed circuit have a great advantage for the intended application since it allows that an abrupt frequency change can be readily detected.

Hence, it is possible to conclude that the designed circuit may be implemented has an EEG frequency tracking monitor.

Unfortunately, there was no time to test the physical circuit with real EEG signals, with different initial VCO frequencies. However, given the concordance observed in single sinusoid signals reported in the previous sections, we believe that the results of Figure 4.4 would be reproduced by the implemented physical circuit.

Chapter 5

Conclusion

5.1 Conclusion

Even though technological advances have allowed the development of new and sophisticated monitoring systems that help anesthesiologists in their day-to-day practice, today's anesthesia monitors' still present some flaws and face some challenges. Their complex algorithms are a reflex of the complexity of the signals that they are analyzing and the neurological processes they try to monitor. And even though they still have many flaws, they also have a promising future ahead.

Most of modern monitors are dependent on the type of drugs used during general anesthesia mostly because specific types of drug have different physiologic effects. Therefore, further knowledge on neurophysiology and pharmacokinetics is needed to develop a highly efficient anesthesia monitor.

Furthermore, current EEG-based monitors are based on feature extraction and classification methods, requiring to be previously trained with a limited database of recorded EEGs. Their algorithms delay the monitors' responses giving the physician a past state of the patient.

The presented technology, based on simple analog systems, unlike other monitors based on digital systems, has a real-time operation, returning results with low time delays.

However, common PLL devices are prepared to operate at higher frequencies and broader bandwidths than an EEG signal. Therefore, to implement this technology as an EEG frequency change tracking device the main goals of this thesis was to adapt this technology to the signals' properties .

First, it was necessary to design a circuit that could have the typical performance of a general PLL but at lower frequencies and small bandwidths. This goal was achieved,

resulting in a circuit that could track frequency changes within a range of ± 55Hz, and withstand abrupt frequency changes of ± 20Hz.

However, the signal had to be previously modulated in order to transform it into a bandpass signal at higher frequencies (between 100 - 147Hz). This was achieved with a VSB modulator associated to a bandpass filter to suppress the carrier and the lower band components. The latter was almost removed, though some vestigial band was still present. The carrier wave could not be removed.

Because of the presence of noise components in the EEG, the PLL circuit had to be associated to a preprocessing subcircuit which included the previously mentioned modulation system and preprocessing filters to isolate the baseband components of the EEG (within 1-47Hz). To achieve this goal, 4th-order filters (high and low pass) were implemented. It was proven that lower order filters would have a poorer performance removing higher frequency components.

In the end, the anesthesia monitor component was not implemented. Due to some technical problems involving the circuit, it was not possible to test with EEGs and different initial VCO frequencies. Nonetheless, it was proven that the designed PLL was able to track EEG frequency changes using single frequency input signals, just like the Simulink model. Thus, we would expect it to also have a similar response in tracking different components according to different initial VCO frequencies.

If the implemented model is proven to operate as expected, then a new low-cost and simple anesthesia monitor may possibly be develop from the proposed methodology.

Current technology and knowledge are far behind the point where a completely reliable depth of anesthesia monitor can be developed. Although, several efforts have been made to improve patients' care during surgical procedures. Newer and more efficient monitors have been developed and anesthesiologists are receiving even more training to rapidly detect any changes in the patients' state.

For now, the final decision about the patient's depth of anesthesia will always be decided by the practitioner.

5.2 Future Work

There is still some work to do in the circuit, specially regarding the preprocessing subcircuit.

First, the circuit needs to be tested using several initial VCO frequencies. Using these tests it is possible to determine a new index based on the PLL's output profiles, through a relation identical to the BIS SynchFastSlow parameter.

Furthermore, a SSB modulation system should be implemented in order to completely remove the carrier's and lower band's components of the AM signal.

A new and better solution to normalize the EEG signal and adapt it to a square wave should be found. Since the signal was amplitude modulated, the designer may develop a system that extracts the signal envelope and, using an analog signal multiplier, try to normalize the signal amplitude against the envelope's amplitude . This solution will be harder to implement if the signal is modulated through a SSB method. The AM-SSB system requires a more complex circuitry to extract the envelope from the signal. On the other hand, the VSB system allows the recovery of the signals envelope using a simple envelope extractor. However, if the VSB is used as the circuit's AM method then the bandpass filter used to suppress the carrier and lower band components should be improved.

The use of a sequential PD may be rethink, since it requires a square wave input. There are to possible approaches: either develop a solution to transform the EEG signal into a square wave or implement an analog mixer to replace the sequential PD. If a normalization system is implemented then the analog mixer's operation will no longer depend on the input signals amplitude.

An important system that may be designed is an artifact detector. During surgery several devices (e.g. electric scalpels and cauterization devices) interfere with the EEG recording instrumentation, introducing more noise components to the EEG signal. It was shown that these devices clearly interfere with the PLL operation leading to erroneous results. The artifact detector would be able to detect these occasional events and remove the EEG epochs affected by the external noise sources.

Bibliography

[1] P. S. Myles, "Prevention of awareness during anaesthesia," *Best Practice and Research: Clinical Anaesthesiology*, vol. 21, no. 3, pp. 345–355, 2007.

[2] C. Lennmarken and G. Sydsjo, "Psychological consequences of awareness and their treatment," *Best practice & research. Clinical anaesthesiology*, vol. 21, no. 3, pp. 357–367, 2007.

[3] L. Voss and J. Sleigh, "Monitoring consciousness: the current status of EEG-based depth of anaesthesia monitors," *Best Practice and Research: Clinical Anaesthesiology*, vol. 21, no. 3, pp. 313–325, 2007.

[4] M. Ghoneim, M, "Incidence of and risk factors for awareness during anaesthesia," *Best Practice and Research: Clinical Anaesthesiology*, vol. 21, no. 3, pp. 327–343, 2007.

[5] C. Prys-Roberts, "Anaesthesia: A practical or impractical construct?" *British Journal of Anaesthesia*, vol. 59, no. 11, pp. 14–16, 1987.

[6] C. Gray, "A reassessment of the signs and levels of anaesthesia," *Irish Jurnal of Medical Science*, vol. 35, no. 11, pp. 499–508, 1960.

[7] D. Griffiths and J. G. Jones, "Awareness and memory in anaesthetized patients," *British Journal of Anaesthesia*, vol. 65, no. 5, pp. 603 – 606, 1990.

[8] P. G. Barash, B. F. Cullen, R. K. Stoelting, M. K. Cahalan, and M. C. Stock, *Handbook of Clinical Anesthesia*, 6th ed. Lippincott Williams & Wilkins, 2006.

[9] N. F. R. D. Lopes, "Monitorização Cerebral Inteligente durante a Anestesia (MONIA)," Master's thesis, Universidade de Coimbra, 2011.

[10] H. Kaul and N. Bharti, "Monitoring depth of anaesthesia," *Indian J. of Anesthesia*, vol. 46, no. 4, pp. 323–332, 2002.

[11] J. Schuttler and H. Schwilden, *Modern Anesthetics*, J. Schuttler and H. Schwilden, Eds. Springer, 2008.

[12] E. R. John and L. S. Prichep, "The anesthetic cascade: a theory of how anesthesia suppresses consciousness." *Anesthesiology*, vol. 102, no. 2, pp. 447–471, 2005.

[13] G. A. Mashour, "Monitoring consciousness: EEG-based measures of anesthetic depth," *Seminars in Anesthesia, Perioperative Medicine and Pain*, vol. 25, no. 4, pp. 205–210, 2006.

[14] J. Snow, "On the Inhalation of the Vapour of Ether in Surgical Operations," Tech. Rep., 1847.

[15] B. L. Douglas, "A Re-evaluation of Guedel ' s Stages of Anesthesia," *Anesthesia Progress*, vol. 5, no. 1, pp. 11 – 14, 1958.

[16] M. Agarwal and R. Griffiths, "Monitoring the depth of anaesthesia," *Anaesthesia and Intensive Care Medicine*, vol. 5, no. 10, 2004.

[17] P. Ray, "Design of ECG-Based Anaesthesia Monitor / Pain Monitor," in *26th Annual International Conference of the IEEE EMBS*. San Francisco: IEEE, 2004, pp. 25–28.

[18] I. J. Rampil, "A primer for EEG signal processing in anesthesia." *Anesthesiology*, vol. 89, no. 4, pp. 980–1002, 1998.

[19] N. Jagadeesan, M. Wolfson, Y. Chen, M. Willingham, and M. S. Avidan, "Brain monitoring during general anesthesia," *Trends in Anaesthesia and Critical Care*, vol. 3, no. 1, pp. 13–18, 2013. [Online]. Available: http://www.sciencedirect.com/science/article/pii/S2210844012001293

[20] Z. Ni, L. Wang, J. Meng, F. Qiu, and J. Huang, "EEG signal processing in anesthesia feature extraction of time and frequency parameters," *Procedia Environmental Sciences*, vol. 8, no. November, pp. 215–220, 2011. [Online]. Available: http://dx.doi.org/10.1016/j.proenv.2011.10.035

[21] J. A. Putman, "Signal Processing Techniques," pp. 1–16, 2007. [Online]. Available: www.eeginfo.com

[22] E. M. Whitham, K. J. Pope, S. P. Fitzgibbon, T. Lewis, C. R. Clark, S. Loveless, M. Broberg, A. Wallace, D. DeLosAngeles, P. Lillie, A. Hardy, R. Fronsko, A. Pulbrook, and J. O. Willoughby, "Scalp electrical recording during paralysis:

Quantitative evidence that EEG frequencies above 20 Hz are contaminated by EMG," *Clinical Neurophysiology*, vol. 118, no. 8, pp. 1877–1888, 2007.

[23] C. Rosow and P. J. Manberg, "Bispectral index monitoring," *Anesthesiology Clinics of North America*, vol. 19, no. 4, pp. 947–966, 2001. [Online]. Available: http://dx.doi.org/10.1016/S0889-8537(01)80018-3

[24] J. W. Johansen, "Update on bispectral index monitoring," *Best practice & research. Clinical anaesthesiology*, vol. 20, no. 1, pp. 81–99, 2006.

[25] J. Bruhn, P. S. Myles, R. Sneyd, and M. M. R. F. Struys, "Depth of anaesthesia monitoring: What's available, what's validated and what's next?" *British Journal of Anaesthesia*, vol. 97, no. 1, pp. 85–94, 2006.

[26] M. S. Avidan, L. Zhang, B. A. Burnside, K. J. Finkel, A. C. Searleman, J. A. Selvidge, L. Saager, M. S. Turner, S. Rao, M. Bottros, C. Hantler, E. Jacobsohn, and A. S. Evers, "Anesthesia Awareness and the Bispectral Index," *The New England Journal of Medicine*, vol. 358, no. 11, pp. 1097–1108, 2008.

[27] S. Kreuer and W. Wilhelm, "The Narcotrend monitor," *Best Practice and Research: Clinical Anaesthesiology*, vol. 20, no. 1, pp. 111–119, 2006.

[28] I. F. Russell, "The Narcotrend 'depth of anaesthesia' monitor cannot reliably detect consciousness during general anaesthesia: An investigation using the isolated forearm technique," *British Journal of Anaesthesia*, vol. 96, no. 3, pp. 346–352, 2006.

[29] B. Bein, "Entropy," *Best Practice & Research Clinical Anaesthesiology*, vol. 20, no. 1, pp. 101–109, 2006.

[30] M. Gruenewald, J. Zhou, N. Schloemerkemper, P. Meybohm, N. Weiler, P. H. Tonner, J. Scholz, and B. Bein, "M-Entropy guidance vs standard practice during propofol-remifentanil anaesthesia: A randomised controlled trial," *Anaesthesia*, vol. 62, no. 12, pp. 1224–1229, 2007.

[31] N. Liu, M. Le Guen, F. Benabbes-Lambert, T. Chazot, B. Trillat, D. I. Sessler, and M. Fischler, "Feasibility of Closed-loop Titration of Propofol and Remifentanil Guided by the Spectral M-Entropy Monitor," *Anesthesiology*, vol. 116, no. 2, pp. 286–295, 2012.

[32] M. Soehle, R. K. Ellerkmann, M. Grube, and C. Med, "Comparison between Bispectral Index and Patient State Index as Measures of the

Electroencephalographic Effects of Sevoflurane," *Anesthesiology*, vol. 109, no. 5, pp. 799–805, 2008. [Online]. Available: http://dx.doi.org/10.1097/ALN.0b013e3181895fd0

[33] D. Drover and H. R. R. Ortega, "Patient state index," *Best Practice and Research: Clinical Anaesthesiology*, vol. 20, no. 1, pp. 121–128, 2006.

[34] M. Soehle, M. Kuech, M. Grube, S. Wirz, S. Kreuer, a. Hoeft, J. Bruhn, and R. K. Ellerkmann, "Patient state index vs bispectral index as measures of the electroencephalographic effects of propofol," *British Journal of Anaesthesia*, vol. 105, no. 2, pp. 172–178, 2010.

[35] G. Schneider, A. W. Gelb, B. Schmeller, R. Tschakert, and E. Kochs, "Detection of awareness in surgical patients with EEG-based indices - Bispectral index and patient state index," *British Journal of Anaesthesia*, vol. 91, no. 3, pp. 329–335, 2003.

[36] C. J. Chisholm, J. Zurica, D. Mironov, R. R. Sciacca, E. Ornstein, and E. J. Heyer, "Comparison of electrophysiologic monitors with clinical assessment of level of sedation." *Mayo Clinic Proceedings*, vol. 81, no. 1, pp. 46–52, 2006.

[37] G. Plourde, "Auditory evoked potentials." *Best Practice & Research Clinical Anaesthesiology*, vol. 20, no. 1, pp. 129–139, 2006.

[38] S. M. Mason, "Evoked potentials and their clinical application," *Current Anaesthesia & Critical Care*, vol. 15, no. 6, pp. 392–399, 2004.

[39] H. Mantzaridis and G. N. Kenny, "Auditory evoked potential index: a quantitative measure of changes in auditory evoked potentials during general anaesthesia," *Anaesthesia*, vol. 52, no. 11, pp. 1030–1036, 1997.

[40] P. A. Pelle, "A Robust Pitch Extraction System Based On Phase Locked Loops," in *31st IEEE International Conference on Acoustics, Speech and Signal Processing (ICASSP)*, 2006, pp. 249–252.

[41] P. Pelle, C. Estienne, and H. Franco, "Robust speech representation of voiced sounds based on synchrony determination with PLLs," in *36th IEEE International Conference on Acoustics, Speech and Signal Processing (ICASSP)*, 2011, pp. 5424–5427.

[42] C. Teixeira, B. Direito, A. Dourado, and F. Sales, "A phase lock loop (PLL) system for frequency variation tracking during general anesthesia," in *IFMBE Preceedings*, vol. 41, 2014, pp. 1527–1529.

[43] P. Lo and Y. Lee, "Applicability of phase-locked loop to tracking the rhythmic activity in EEGS," *Circuits, Systems and Signal Processing*, vol. 19, no. 3, pp. 171–186, 2000.

[44] A. B. Carlson, P. B. Crilly, and J. C. Rutledge, *Communication systems: An introduction to Signals and Noise in Electrical Communication*, 4th ed. New York: McGraw-Hill, 2002. [Online]. Available: http://scholar.google.com/scholar?hl=en&btnG=Search&q=intitle:Communication+Systems#3

[45] F. M. Gardner, *Phaselock Techniques*. Wiley, 2005.

[46] R. E. Best, *Phase-Locked Loops - Design, Simulation and Applications*, 5th ed. McGraw-Hill, 2003.

[47] D. H. Wolaver, *Phase-Locked Loop Circuit Design*. New Jersey: Prentice Hall, 1991.

[48] S. Long, "Phase Locked Loop Circuits," UCSB, Tech. Rep., 2005.

[49] D. Banerjee, "PLL Fundamentals," Tech. Rep., 2011.

[50] A. S. Nandini, "Design and Implementation of Analog Multiplier with Improved Linearity," *International Journal of VLSI design & Communication Systems*, vol. 3, no. 5, pp. 93–109, 2012.

[51] D. H. Sheingold, "Multiplier Application Guide," 1978.

[52] K. W. Whites, "Lecture 27 : Mixers - Gilbert Cell," Tech. Rep., 2006.

[53] L. Moura, *Apontamentos de Electrónica III*, 1st ed. Faro: Universidade do Algarve, 2003.

[54] P. E. Allen, "Lecture 110 – phase frequency detectors," Tech. Rep., 2003.

[55] A. C. Kailuke, P. Agrawal, and R. V. Kshirsagar, "Design of Phase Frequency Detector and Charge Pump for High Frequency PLL," in *2014 International Conference on Electronic Systems, Signal Processing and Computing Technologies*, 2014.

[56] J. Wilkin, "Voltage Controlled Oscillators," University of Toronto, Tech. Rep., 2001.

[57] H. R. Carmezind, "Redesigning the old 555," *IEEE Spectrum*, no. September, pp. 80–85, 1997.

[58] "555 Oscillator Tutorial." [Online]. Available: http://www.electronics-tutorials.ws/waveforms/555_oscillator.html

[59] R. Marston, "Miscellaneous 555 circuits," in *Timer/Generator Circuits Manual*, 1990, pp. 226–253. [Online]. Available: http://linkinghub.elsevier.com/retrieve/pii/B9780434912919500164

[60] A. S. Sedra and K. C. Smith, *Microelectronic Circuits*, 5th ed., 2004.

[61] T. I. Inc., "TLC555 LinCMOS Timer - Datasheet," Dallas, pp. 1–17, 2005.

[62] V. O. Sannibale, *Analog Electronics - Resonant Circuits*, 2012.

[63] A. D. Berny, "Analysis and Design of Wideband LC VCOs," Master's thesis, University of California, 2006.

[64] B. Razavi, "Basic LC VCOs," Electrical Engineering Department University of California, Los Angeles, Tech. Rep.

[65] X. Zhao, R. Chebli, and M. Sawan, "A wide tuning range voltage-controlled ring oscillator dedicated to ultrasound transmitter," in *The 16th International Conference on Microelectronics (ICM 2004)*, 2004, pp. 313–316.

[66] G. Flewelling, "An Analog Phase-Locked Loop," University of Maine, Tech. Rep., 2014.

[67] A. Devices, "Chapter 2: Other Linear Circuits," in *Basic Linear Design*, analog dev ed. Analog Devices, 2008, ch. 2, p. 943.

[68] A. Dourado, "Dinâmica dos Sistemas Biológicos e Fisiológicos - Notas de Apoio da disciplina de Modelos Computacionais dos Processos Fisiológicos," 2011.

[69] B. W. Li, "Introduction to phase-locked loop system modeling," *Analog Applications*, vol. 1, no. May, pp. 5–11, 2000. [Online]. Available: http://application-notes.digchip.com/001/1-1109.pdf#page=9

[70] N. Sharma, M. Trikha, and V. Rajpoot, "A Novel Approach for Single Sideband Modulation using Hilbert Transform," *MIT International Journal of Electrical and Instrumentation Engineering*, vol. 2, no. 2, pp. 102–105, 2012.

[71] A. Devices, "Chapter 8: Analog Filters," in *Basic Linear Design*, 2008, p. 943.

[72] A. Basit, W. Aziz, and F. Zafar, "Implementation of SSB Modulation / Demodulation using Hilbert Transform in MATLAB," *Journal of Expert Systems (JES)*, vol. 1, no. 3, pp. 79–83, 2012.

[73] B. P. Lathi, *Modern Digital and Analog Communication Systems*, 1998. [Online]. Available: http://portal.acm.org/citation.cfm?id=541365

[74] M. A. E. Ramsay, T. M. Savege, B. R. Simpson, and R. Goodwin, "Controlled sedation with alphaxalone-alphadolone." *British Medical Journal*, vol. 2, no. 5920, pp. 656–659, 1974.

Appendix A

Modern DOA Classification Scales

Table A.1: Ramsay's Scale of Sedation [74]

Assessment	Score
Patient is anxious and agitated or restless or both	1
Patient is cooperative, oriented and tranquil	2
Patient responds to commands only	3
Patient exhibits active response to light glabellar tap or loud auditory stimulus	4
Patient exhibits a slow response to light glabellar tap or loud auditory stimulus	5
Patient exhibits no response	6

Table A.2: Modified Observer's Assessment of Alertness/Sedation Scale (MOAA/SS) [11]

Score	Responsiveness	Speech	Facial Expression	Eyes
5	Responds readily to name spoken in normal tone	Normal	Normal	Clear, no ptosis
4	Lethargic response to name spoken in normal tone	Mild slowing or thickening	Mild relaxation	Glazed or mild ptosis (less than half of the eye)
3	Responds only after name is called loudly and/or repeatedly	Slurring or prominent slowing	Marked relaxation (slack jaw)	Glazed and marked ptosis (half of the eye or more)
2	Responds only after mild prodding or shaking	Few recognizable words	-	-
1	Does not respond to mild prodding or shaking	-	-	-
0	Does not respond to pain	-	-	-

Appendix B

Preprocessing Filters

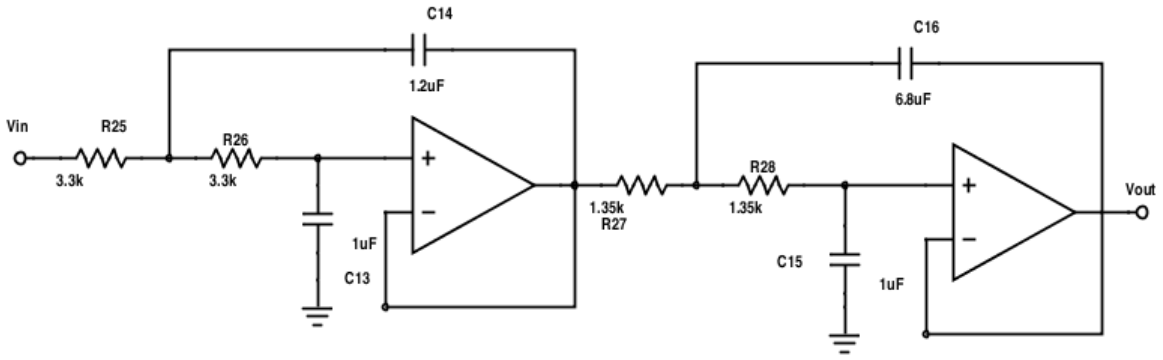

Figure B.1: Preprocessing Low-Pass Filter

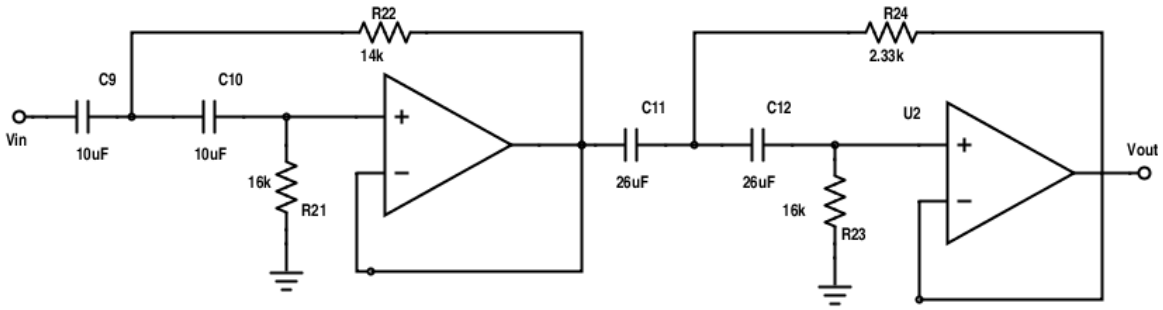

Figure B.2: Preprocessing High-Pass Filter

Appendix C

Amplitude Modulator Bandpass Filter

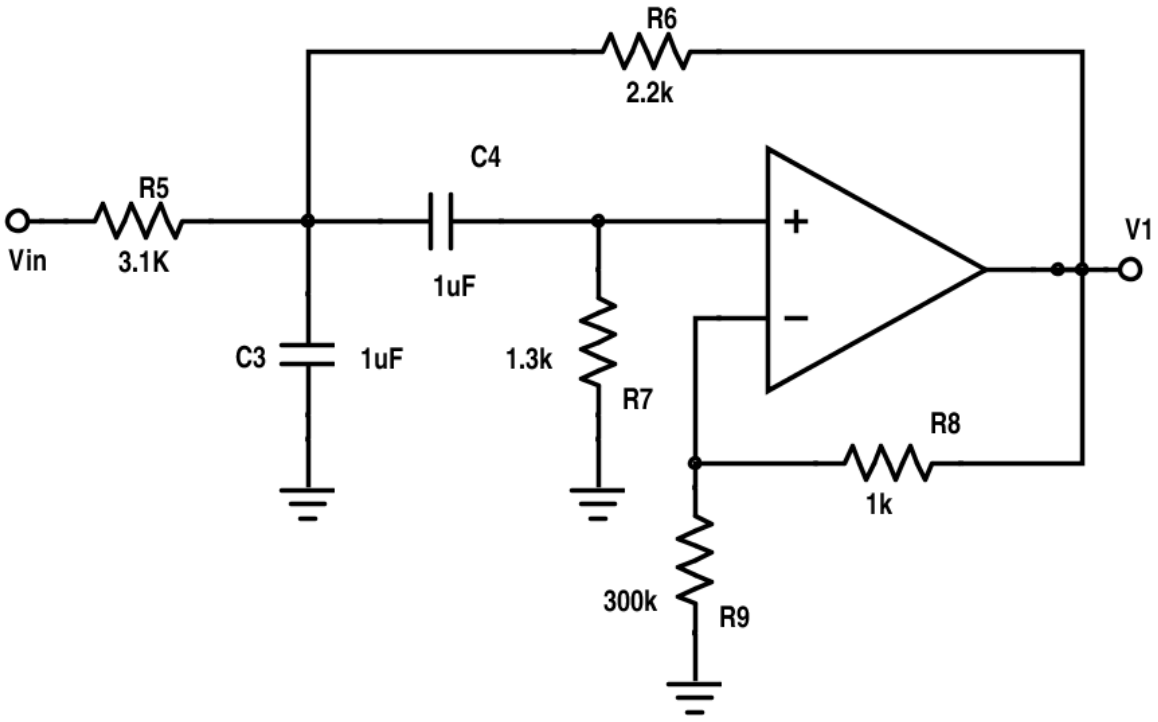

Figure C.1: VSB system Bandpass Filter Stage 1

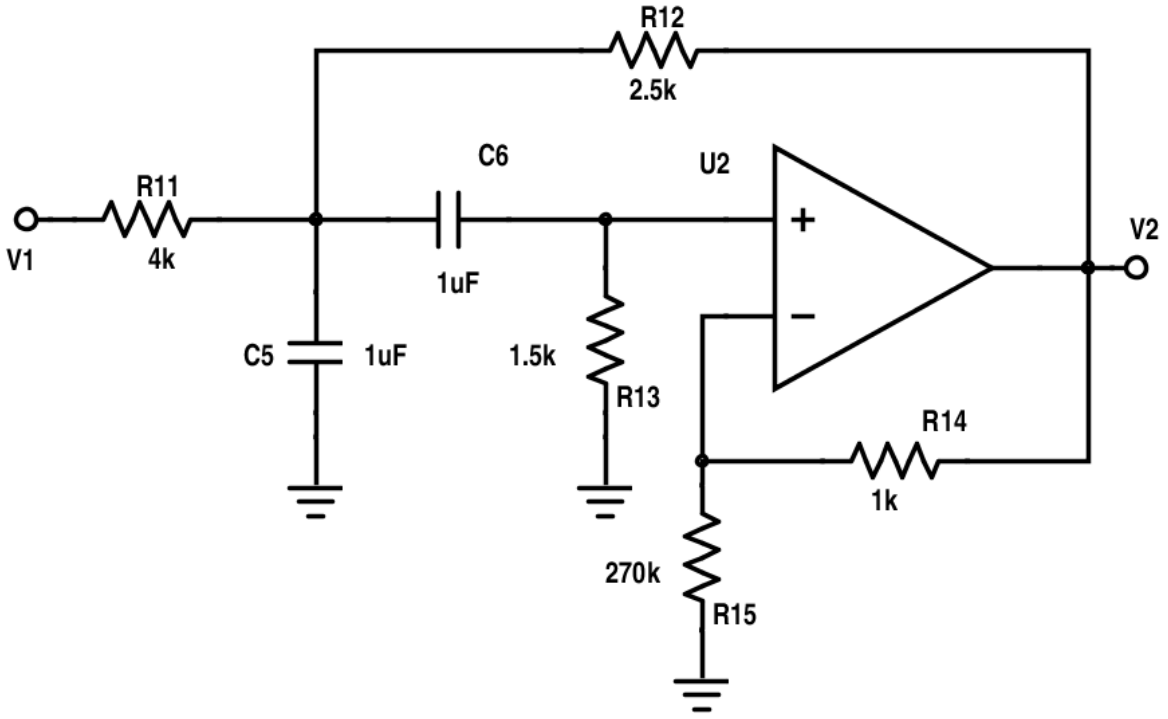

Figure C.2: Bandpass Filter Stage 2

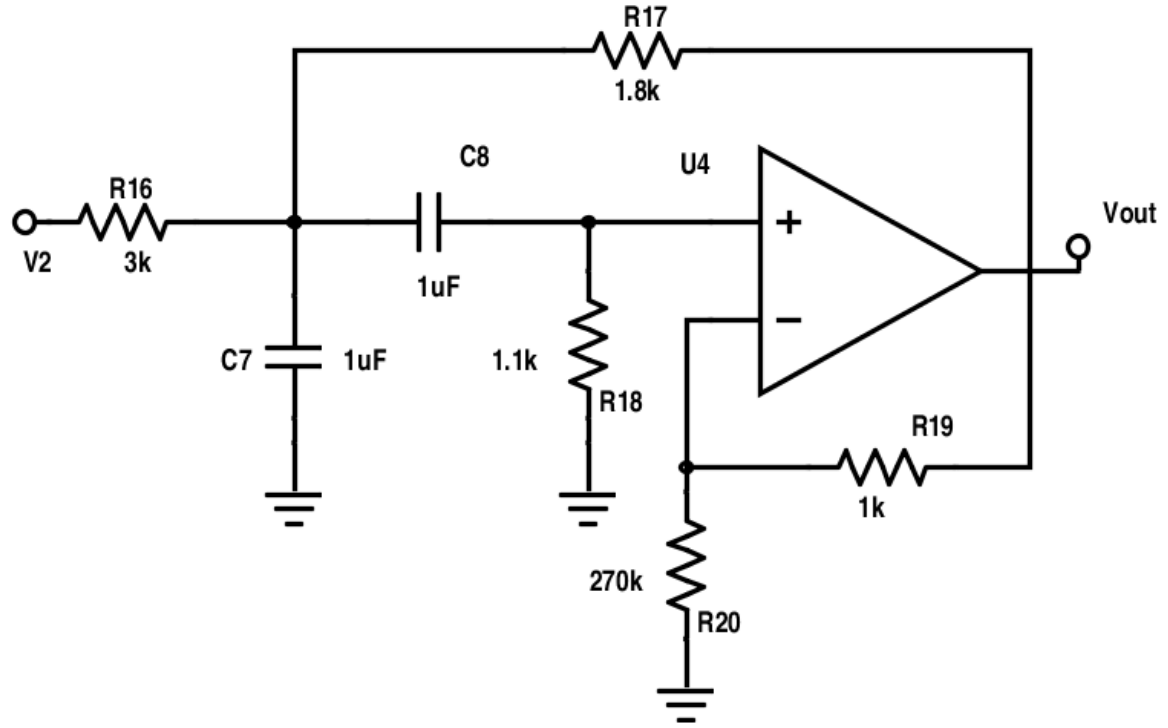

Figure C.3: Bandpass Filter Stage 3

Appendix D

The Analog PLL

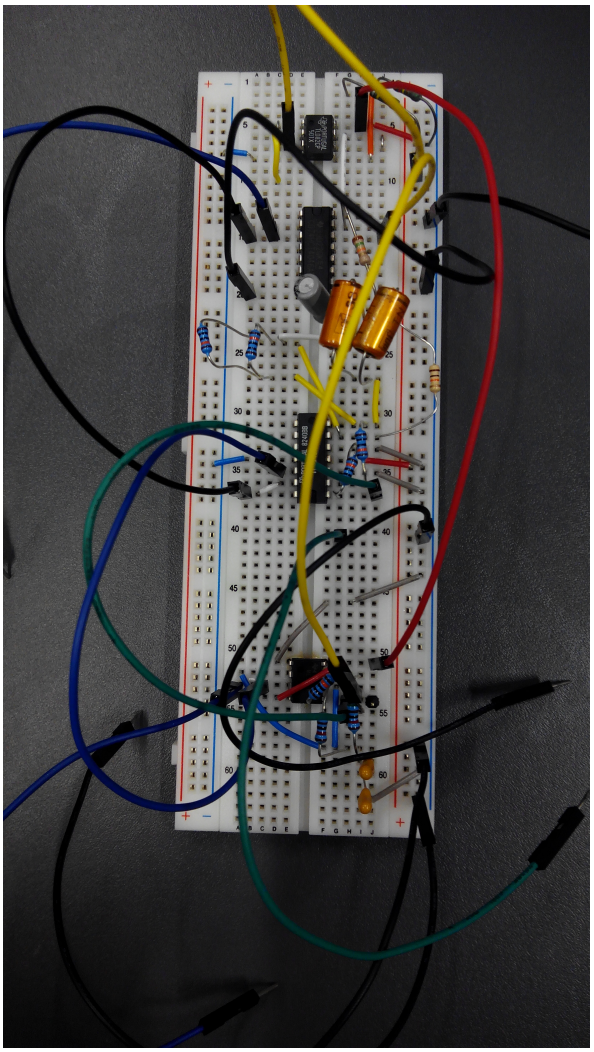

Figure D.1: Final implementation of the designed analog circuit.